NOTE TO USERS

This reproduction is the best copy available.

uOttawa

L'Université canadienne
Canada's university

FACULTÉ DES ÉTUDES SUPÉRIEURES ET POSTDOCTORALES

uOttawa

L'Université canadienne
Canada's university

FACULTY OF GRADUATE AND POSTDOCTORAL STUDIES

Nazir Kabbani

AUTEUR DE LA THÈSE / AUTHOR OF THESIS

M.Sc. (Biochemistry)

GRADE / DEGREE

Department of Biochemistry, Microbiology and Immunology

FACULTÉ, ÉCOLE, DÉPARTEMENT / FACULTY, SCHOOL, DEPARTMENT

Chemical-Genetic Profiling of Platelet-Activating Factor in Yeast

TITRE DE LA THÈSE / TITLE OF THESIS

K. Beatz

DIRECTEUR (DIRECTRICE) DE LA THÈSE / THESIS SUPERVISOR

CO-DIRECTEUR (CO-DIRECTRICE) DE LA THÈSE / THESIS CO-SUPERVISOR

EXAMINATEURS (EXAMINATRICES) DE LA THÈSE / THESIS EXAMINERS

A. Golshani

J. Lee

Gary W. Slater

Le Doyen de la Faculté des études supérieures et postdoctorales / Dean of the Faculty of Graduate and Postdoctoral Studies

CHEMICAL-GENETIC PROFILING OF PLATELET-ACTIVATING FACTOR IN YEAST

by

Nazir Kabbani

Student Number 2790288

Submitted in partial fulfillment
of the requirements for the degree of
Master of Science
Faculty of Graduate Studies

SFU
Department of Biochemistry, Microbiology, and Immunology
Faculty of Medicine
The University of Ottawa
Ottawa, ON

07 June 2009

Your file Votre référence
ISBN: 978-0-494-58218-3
Our file Notre référence
ISBN: 978-0-494-58218-3

ABSTRACT

The basic biological processes between the yeast *Saccharomyces cerevisiae* and mammals are highly conserved. Yeast posses many genes that are implicated in human diseases and have been successfully used as a model for the study of neurodegeneration. Platelet-Activating Factor (C16:0 PAF) causes neuronal cell death independent of its receptor and has been implicated in Alzheimer's disease. I hypothesized that yeast could be used as a model system for deciphering PAF receptor-independent signalling and have utilized genome-wide chemical genomic screening in yeast to further characterize the molecular mechanism of PAF toxicity. Two complementary screens implicate PAF in many cellular processes, some of which parallel results obtained in mammalian studies. I have found that PAF challenge is cytotoxic, delays cell cycle progression, and affects actin stability leading to spindle misorientation and bi-nucleate mother cells.

ACKNOWLEDGEMENTS:

The wisdom and instruction of many people has contributed to this thesis. My supervisor, Dr. Kristin Baetz, was instrumental in her guidance, funding, and assessment of my progress during my master's project. Her patience and thrust kept me moving forward. The first contribution to this work came from Eric Imbeault-Fréchette (summer student) who had started this project by performing the first replica of one of the screens and had also determined empirically the ideal concentrations to use for that screen. As for the lipidomics work, I thank Dr. Shawn Whitehead for performing the lipid extractions on my samples and Weimin (David) Hou for running those samples on the Mass Spectrometer. The two of them, along with Leigh Anne Swayne taught me how to analyze the data using Analyst software. Ying Fong helped greatly in the development of a computerized scoring method for the screens. I also thank my thesis advisory committee members (Dr. Adam Rudner, Dr. Steffany Bennett, and Dr. Daniel Figeys) for their insight and critical assessment which has allowed me to improve as a researcher. Leslie Mitchell deserves special thanks for her help in training me on many protocols used in the lab. I thank all the lab members of the Baetz Lab: Leslie Mitchell, Maria Gerdes, Sharon Berthelet, Winnie Chen, Ying Fong and Andrea Lau. As for others in the department, I would like to thank Sujeeve Jeganathan for thoughtful discussions of my protocols and data as well providing me with the alexa-fluor antibody.

I would like to thank my parents (Mona and Mahmoud Kabbani) and sister (Alaa Kabbani) for their continual support as well as my wife (Zeinab Tannir) for her strong encouragement and love.

TABLE OF CONTENTS

LIST OF ABBREVIATIONS

DNA	Deoxyribonucleic Acid
ORF	Open Reading Frame
PCR	Polymerase Chain Reaction
SDS	Sodium-Dodecyl Sulfate
SGA	Synthetic Genetic Array
SSL	Synthetic Lethal (SL) or Synthetic Sickness (SS)
YPD	Yeast Peptone Dextrose
PAF	Platelet-Activating Factor
L-PAF	lysoPlatelet-Activating Factor
PAFR	Platelet-Activating Factor Receptor
PC	Phosphatidylcholine
LPC	lysoPhosphatidylcholine
PA	Phosphatidic acid
LPA	lysoPhosphatidic acid
PLA2	phospholipase A2
PAF-AH	Platelet-Activating Factor acetylhydrolase
L-PAF-AT	lysoPlatelet-Activating Factor acetyltransferase
CFU	Colony Forming Units
Htt	Huntingtin protein
HD	Huntington Disease
AD	Alzheimer's Disease
PD	Parkinson's Disease

LIST OF FIGURES

LIST OF TABLES

CHAPTER 1: INTRODUCTION

A link between the neurodegenerative Alzheimer's Disease (AD) and lipids has been found (1-4). It is increasingly being demonstrated that lipids act as second messengers and signalling molecules. One such bioactive lipid, platelet-activating factor (PAF), was first identified by its ability to cause platelet aggregation, but is now known to also cause neuronal cell death independent of its receptor. As well, it has been implicated in Alzheimer's disease progression (1, 2, 5-11). The molecular mechanism of PAF-dependent neuronal toxicity is not known.

The budding yeast *Saccharomyces cerevisiae* has been successfully used as a model for the study of neurodegenerative diseases such as Alzheimer's (12-18). In this study I hypothesized that yeast could be used as a model system for studying PAF receptor-independent signalling and have performed genome-wide chemical-genomic screening to identify proteins and pathways that upon deletion enhance PAF toxicity. Overall, this study demonstrates that two-unbiased and complementary screens produced a chemical-genetic profile that implicates PAF in many cellular processes, including pathways previously linked to Alzheimer's disease. This study indicates that yeast chemical-genomic screens are a potentially valuable tool in elucidating the cellular role of PAF and similar lipids in Alzheimer's progression.

1.1 Yeast As A Model Organism For Amyloidoses

Saccharomyces cerevisiae has been widely employed as a model system for studying many aspects of biology found in higher eukaryotes including cell division, DNA repair, protein folding, and trafficking (reviewed in 19, 20-24). The reasons for this choice are many, and include the power of yeast's classical genetics tools (reviewed in 25), a sequenced genome (26) with extensive annotation (27, 28) and ease of directed mutagenesis that allowed for the systematic creation of deletion mutants and overexpression libraries (29, 30). More importantly, the basic biological processes between yeast and man are highly conserved and yeast posses many genes that are implicated in human diseases (31-34).

Though historically used as a model for cancer due to the conservation of the cell cycle machinery (35, 36), yeast has recently been successfully used as a model for the study of neurodegenerative diseases such as Alzheimer's, Parkinson's and Huntington's (12-18). These diseases are termed "amyloidoses" due to their common underlying protein misfolding and aggregation characteristics. Here, I discuss the yeast models that were developed for the study of Parkinson's, Huntington's, prion, and Alzheimer's disease.

In Parkinson's disease (PD), accumulation of Alpha-synuclein forms Lewy Bodies (abnormal aggregates of protein) inside neurons. This accumulation is thought to cause the disease pathogenesis by displacing cellular compartments and inhibiting ER-Golgi traffic (37-39). Yeast was used as a model system to investigate Alpha-synuclein toxicity (16, 17, 39). Using GFP-tagged Alpha-synuclein, the localization of mutant forms compared to wildtype was determined. The localization for these constructs was

consistent with other model systems in that wildtype Alpha-synuclein concentrated at the plasma membrane. Cells with two copies of wildtype Alpha-synuclein showed cytoplasmic aggregates. Also, one of the mutants behaved like wildtype while the other mutant showed a cytoplasmic localization that was diffuse and consistent with its weak ability to bind the membrane in other systems (16). These constructs were also used for observing the effect of overexpression of Alpha-synuclein and it was found that, similar to mammalian cells, overexpression of Alpha-synuclein caused large cytoplasmic inclusions and inhibited phospholipase D activity in yeast thus validating the use of yeast as a PD model. This finding also validated the hypothesis that accumulation of Alpha-synuclein overloads the cell's quality control system for protein folding and causes the disease related-toxicity (16). Additionally, a screen for genome-wide yeast mutants that enhance Alpha-synuclein toxicity was performed by synthetic-lethal Synthetic Genetic Array (SL-SGA) methodology (17). SL-SGA is a genetic tool that allows for the systematic construction of double mutants between a mutant of interest and all non-essential deletion mutants (roughly 4000) in yeast (See below, 40). This screen was performed to assess the level of toxicity of Alpha-synuclein expression in each non-essential deletion mutant in yeast. It was found that 86 deletion mutants display either a growth defect or death upon expression of Alpha-synuclein. The mutants identified were enriched for genes encoding proteins involved in lipid metabolism and vesicle-mediated transport (17). The use of yeast as a PD model is not only feasible but also yields novel results that portray an accurate picture of the underlying biology of the disease.

A similar screen was also performed to find enhancers (17) and suppressors (41) of an Huntingtin (Htt) mutant fragment toxicity. Htt is a gene that codes for a 348 kDa

protein called "Huntingtin protein" and the normal functions of Htt are not fully known (42). It seems to play a role in neurons and has the highest expression levels in the brain. It is however also needed for the development of the embryo (43). Mutants of Htt that contain an abnormal number (36+) of glutamines at the N-terminal are fragmented by the cell's machinery and form abnormal inclusions that lead to the disease pathogenesis. The Htt yeast screen found that the strongest suppressor of toxicity was a gene that encodes kynurenine 3-monooxygenase. The kynurenine pathway is the main route for tryptophan degradation in eukaryotes. This pathway is activated in HD affected patients and in animal models as well. This highlights the relevance of the yeast model (41) and suggests a conservation of the mechanism of toxicity. The genes that were identified in the Huntingtin screen were different from those of the Alpha-synuclein screen (mentioned above) with an overlap of only one gene; this points toward specificity in the yeast model.

A screen for identifying compounds acting against yeast prions has also been developed in yeast (12, 13). Remarkably it was found that the compounds isolated in the yeast screen also inhibited mammalian prion formation. This illustrates that yeast and man share common biological processes that impact prions. In addition, yeast prions have been used to study amyloid polymerization inhibitors (14). Given the above, it is clear that yeast can be used to study many different aspects of amyloidoses.

In AD, the accumulation of Amyloid-β (Aβ) plays a major part in disease progression. Aβ is made from cleavage of the transmembrane amyloid precursor protein (APP) by specific secretases (reviewed in 37). To aid in the identification of the human secretases, a yeast model expressing APP was used to identify secretases that cleave APP

(18). The study identified two secretases in yeast capable of cleaving APP and rightfully concluded that aspartyl proteases are good candidates to narrow down the search in humans (18). It can be readily appreciated that identification of inhibitors that act specifically on these secretases has great therapeutic potential. A screen to find inhibitors of a human secretase expressed in yeast was developed such that it identified compounds that not only inhibit the human enzyme but also crossed cellular membranes without being cytotoxic (15). This screen employed a *lacZ* reporter assay and 15,000 compounds and had identified 13 secretase inhibitors (15). These results highlight the speed and ease of working with the yeast model and its overall applicability to the study of amyloidoses.

1.2 Lipid Second Messengers

The central theme in biology that "structure serves function" leads to the question of why cells produce thousands of different lipid species. It is generally accepted that lipids play three major roles: 1) energy storage 2) compartmentalization as membrane components and 3) signalling as first and second messengers (reviewed in 44). Energy is stored mainly as triacylglycerol or steryl esters while the major structural lipids in eukaryotic membranes are glycerophospholipids such as phosphatidylcholine, which notably accounts for greater than half of the phospholipids in these membranes (reviewed in 44, 45). Membrane phospholipids are composed of predominantly 16 or 18 carbon fatty acid chains and are given the nomenclature Cx:y, where x is the number of carbons on the sn-1 position chain and y is the number of double bonds in that chain (46).

Communication between cells is crucial and usually involves a signal or stimulant that is detected and then transmitted across the plasma membrane boundary. The plasma membrane not only serves as a mechanical barrier but also as a pool for second

messenger lipids which are usually found at much lower concentrations than other membrane lipids (47). Second messenger lipids can act by binding cell surface receptors that activate downstream factors or that activate lipid metabolizing enzymes that release the messengers' head-groups inside the cell to activate effectors such as kinases. One such example is diacylglycerol (DAG) which activates protein kinase C by binding to its allosteric site (48). Phosphatidylcholine can be broken down by phospholipase D and the resulting phosphatidic acid (another signalling molecule) is recycled back to DAG (49, 50). Phosphatidic acid can activate calcium channels and inhibit adenylyl cyclase. In this way, phosphatidylcholine and other lipids such as phosphatidylinositol in the plasma membrane provide a plentiful supply of substrates via the action of phospholipases and sphingomyelinases. One can thus appreciate the vitality of temporal and spatial regulation of such molecules in the membrane and its impact on disease states (4).

1.3 Actin And Spindle In Yeast

The regulation and remodelling of actin networks in yeast is crucial for processes such as endocytosis, spindle orientation, and cytokenisis. The actin protein is about 42-kDa and, in yeast, is expressed from one essential gene (*ACT1*) the proteins of which (termed G-actin) polymerize to form filaments having a barbed (+) end and a pointed (-) end (termed F-actin). In yeast, there are three F-actin structures termed patches, rings, and cables (reviewed in 51). Actin patches are localized cortically at sites of polarized growth, are highly motile, and are involved in endocytosis as they are physically linked with clathrin patches at the cortex (reviewed in 51). The structure of an actin patch is proposed to be a branched network of filaments arranged in a cone shape around a finger-like invagination in the plasma membrane with the *ARP2/3* complex (the actin nucleator)

at the tip of the cone (52). Actin cables on the other hand are used to transport cargo in the cell and assemble in an *ARP2/3*-independant manner with the help of formins (Bni1p and Bnr1p). Cables are composed of short filaments arranged unidirectionally into bundles surrounded with tropomyosin (filament stabilizer) such that the barbed ends (providing fast growth) orient towards polarity sites.

In order for chromosomes to separate correctly in dividing cells there needs to be coordination between cell polarity cues, mitotic spindle orientation, and cell cycle checkpoints. In yeast, spindle forms in between spindle pole bodies (SPB) found in the nuclear envelope and are composed of tubulin (*TUB1-4*) dimers that form microtubules (53). From the SPBs emanate the astral microtubules towards the cell periphery and are used to aid in the spindle orientation process. There are two pathways in yeast for spindle orientation: dynein pathway and Kar9 pathway (reviewed in 54). The Kar9 and Dynein pathways are parallel pathways in that the loss of both is lethal (55). In the Kar9 pathway, the spindle orient by attaching astral microtubules to actin cables extending from the bud via Kar9p and Myo2p (reviewed in 54, 56). Myo2p is the motor that provides the force needed to orient the spindle by moving astral microtubules along actin cables emanating from the bud (reviewed in 57). In the Dynein pathway, the dynein complex localizes to the ends of astral microtubules and pulls the spindle through the bud neck by attaching to Num2p (the cortical anchor). The dynactin complex is required for dynein activity (55). The Kar9 pathway occurs prior to anaphase while the dynein pathway takes place during anaphase. In order to ensure that the cell cycle does not progress until the spindle are oriented properly and the nuclear envelop has gone through the bud neck, cells use the spindle position checkpoint (SPOC). The SPOC inhibits mitotic exit and cytokinesis. The

SPOC's directly inhibits Tem1p by binding of Bub2p/Bfa1p. Tem1p activation by Lte1p is needed to progress out of mitosis (reviewed in 54) however, Tem1p and Lte1 are physically separated as Tem1p is found in the mother cell while Lte1 is in the bud. It has been proposed that these two proteins only meet when the nuclear envelope has gone through the bud neck in late anaphase indicating a properly positioned spindle (58).

1.4 PAF Is A Bioactive Lipid Implicated In Alzheimer's Disease

Platelet-Activating Factor (PAF), also known as PAF, PAF-acether or AGEPC (acetyl-glyceryl-ether-phosphorylcholine), is defined by an alkyl-ether linkage at the sn-1 position, an acetyl group at the sn-2 position, and a phosphocholine at the sn-3 position (46) (Figure 1). PAF is a family of bioactive lipids with varying sn-1 chain lengths and each confers different cellular effects. PAF was originally found as a phospholipid mediator released by sensitized rabbit basophils and aggregated platelets at low concentrations during IgE-mediated anaphylaxis in rabbits (59). Since its discovery, studies on PAF have indicated that it has many functions at physiological levels (nM range) and yet others at pathophysiological levels (μM range) in diseases and during injury. At physiological levels, it acts through its membrane receptor and is involved in

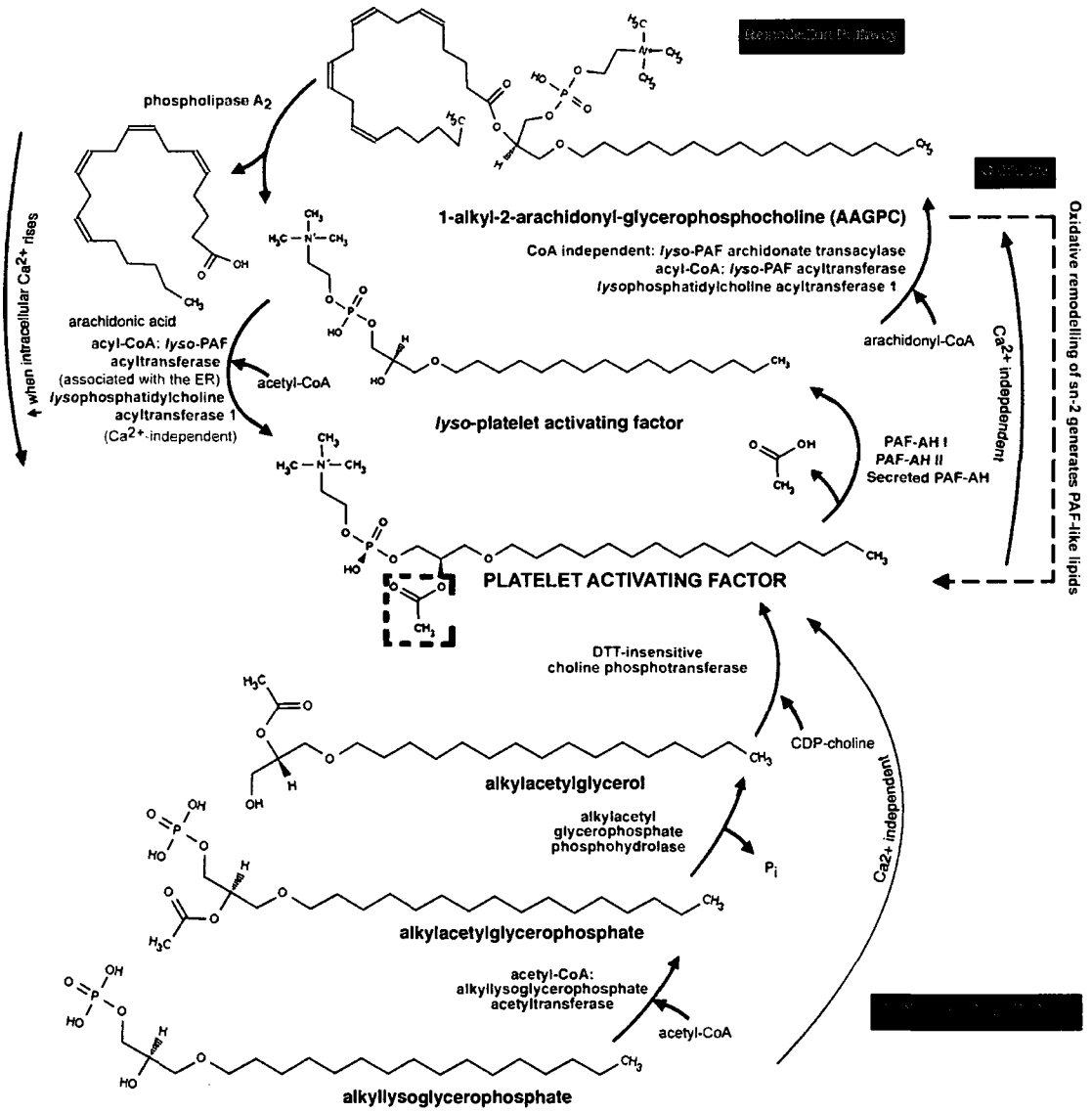
phospholipase A2
1-alkyl-2-arachidonyl-glycerophosphocholine (AAGPC)
CoA independent: lyso-PAF archidonate transacylase
acyl-CoA: lyso-PAF acyltransferase
lysophosphatidylcholine acyltransferase 1
arachidonyl-CoA
Ca2+ independent
Oxidative remodelling of sn-2 generates PAF-like lipids
when intracellular Ca2+ rises
arachidonic acid
acyl-CoA: lyso-PAF acyltransferase (associated with the ER) lysophosphatidylcholine acyltransferase 1 (Ca2+-independent)
acetyl-CoA
lyso-platelet activating factor
PAF-AH I
PAF-AH II
Secreted PAF-AH
PLATELET ACTIVATING FACTOR
DTT-insensitive choline phosphotransferase
CDP-choline
alkylacetylglycerol
alkylacetyl glycerophosphate phosphohydrolase
Pi
alkylacetylglycerophosphate
acetyl-CoA: alkyllysoglycerophosphate acetyltransferase
acetyl-CoA
alkyllysoglycerophosphate
Ca2+ independent

Figure 1. Platelet Activating Factor Metabolic Pathways. Three main pathways produce the PAF family of glycerolipids. Red: The remodelling pathway is the primary enzymatic pathway for PAF production. Blue: The de novo synthesis pathway used to make basal levels of PAF. Green: non-enzymatic oxidation of membrane lipids to produce PAF-like lipids with sn-2 position (hatched green box) fatty acid chains up to 8 carbons. This schematic depicts C16-PAF synthesis from the 1-alky-2-arachidonyl-glycerophosphocholine precursor lipid. Adapted with permission from Ryan SD, Harris CS, Carswell CL, Baenziger JE, Bennett SAL (2008) Heterogeneity in the sn-1 carbon chain of platelet activating factor glycerophospholipids determines pro-or anti-apoptotic signaling in primary neurons. J Lipid Res, 49:2250-2258. (60).

asthma, inflammation, allergic response, and shock (reviewed in 61). Further, it is involved in bronchial hyperactivity (62) and anaphylaxis (63). Mammalian studies of PAF show a link between PAF and F-actin polymerization/depolymerization oscillations (64-66). Thimidine uptake assays have demonstrated that PAF impinges upon cell proliferation (67-69); and mice overexpressing the PAF receptor develop skin tumors (62). This indicated a role for PAF in cell cycle regulation. Other functions include the mediation of intercellular interaction and cell-cell adhesion (reviewed in 46).

In the brain, PAF is thought to mediate functions ranging from synaptic transmission and plasticity to neuroprotection (reviewed in 70). As well, it is a retrograde neurotransmitter involved in long-term potentiation (71, 72). At high levels in the brain PAF becomes neurotoxic and mediates cell loss in many diseases (5, 7-11, 61, 73-78). For example, HIV-1 infection of the nervous system causes an increased release of PAF by infected monocytes inducing neuronal apoptosis. The neuronal apoptosis in this condition was prevented by PAF degrading enzymes (PAF-AHs discussed below) and is thought to occur through the PAF receptor (73). Further, PAF also mediates apoptosis of neurons in conditions such as epileptic seizure (75). It is clear that PAF plays a crucial role in the brain and high levels of it have been found in neurodegenerative disorders. For example, higher enzymatic activity (phospholipase A2 discussed below) was elicited by Aβ oligomerization and lead to high levels of bioactive glycerophospholipids including PAF (reviewed in 1-4, 5, 6, 76). In addition, it has been found that shifting the composition of fatty acids in synaptosomal phosphatidylcholines from octadecyl (18:0) to hexadecyl (16:0) species by dietary means impinges on the timing of Alzheimer's disease

onset (79). This highlights the importance of the sn-1 chain length in determining the exact effect of each PAF species in relation to diseases.

C16:0 PAF toxicity can occur through an unknown PAF-receptor (PAFR)-independent pathway (80). This toxicity is, in some cases, caspase-dependant and can occur with or without the receptor depending on the PAF species (C16 or C18) (60). Also, C16:0 PAF was again implicated in Alzheimer's disease by acting downstream of Aβ and by enhancing Aβ oligomerization (reviewed in 1, 2, 4, 5).The lack of knowledge about the receptor-independent signalling pathway indicates that studies into C16:0 PAF's involvement in neurotoxicity are warranted.

1.5 PAF Biosynthesis Pathways

PAF biosynthesis occurs via three main pathways. 1) *de novo*. 2) Remodelling. 3) Oxidative remodelling (Figure 1). The first two pathways are regulated and each is responsible for different levels of PAF and PAF-like lipids. The remodelling pathway simply substitutes an acetyl group at the sn-2 position for the existing acyl fatty-acid chain of other phospholipids. This is done via a two step calcium-dependent process. Rises in intracellular calcium triggers phospholipase A_2 (PLA_2) to remove the fatty acid chain at the sn-2 of precursor phospholipids to create lyso-PAF (L-PAF) which is then acetylated by the calcium-stimulated lyso-platelet activating factor acetyl-transferase (L-PAF-AT) to produce PAF (81, 82). L-PAF-AT has been found in both humans and yeast despite the lack of sequence similarity (81, 83). The reverse direction of this pathway is calcium independent. The acetyl group of PAF is hydrolyzed by PAF acetylhydrolases (PAF-AH) thus producing L-PAF which is then reacylated by a transacylase (84) or lysophospholipase D (85). This remodelling pathway contributes to the majority of PAF

produced during inflammation while the *de novo* pathway makes PAF at physiological levels for normal cellular function (46). The *de novo* pathway has three steps and starts with a molecule that has an alkyl at the sn-1 position (1-alkyl-2-lyso-glycero-3-P). This precursor is acetylated at the sn-2 and then the phosphate at the sn-3 is removed to be replaced with phosphocholine derived from CDP-Choline (86). Finally, PAF-like lipids are produced via the non-enzymatic oxidative remodelling of membrane lipid. For example, oxidation of an unsaturated phosphatidylcholine at the sn-2 may produce PAF-like molecules that have up to 8 carbons at the sn-2 instead of the acetyl group of PAF (87, 88)

With the exception of PAF-like lipid production, PAF biosynthesis pathways are regulated. This tight control is achieved through many mechanisms that include enzymatic control of synthesis, constitutively expressed degradative enzymes, and regulated PAF-receptor (reviewed in 89). For example, the receptor's expression is controlled by cytokines and by intracellular cAMP levels (90).

1.6 PAF In Yeast

Presently, our knowledge of PAF in yeast is limited. Varying C16:0 PAF levels have been found in many different yeast strains of the genus *Saccharomyces* (91, 92) with the highest levels found in stationary cells (93). It also appears that PAF levels may be cell cycle regulated with higher levels of C16:0 PAF in G1 or M compared to S-phase (93). It was also shown that up to 10-fold increases in yeast C16:0 PAF can be elicited by treatment with the calcium ionophore A23187 in a time and concentration dependant manner suggesting that C16:0 PAF synthesis in yeast occurs through the Ca^{2+}-dependent remodelling pathway (93, 94). Interestingly, PAF production in yeast is temperature

dependant with lower levels at 14°C than at 20°C (92). Other yeast genera were tested for PAF but the majority showed no detectable PAF levels (91). The presence of PAF in *Saccharomyces* indicates that an enzymatic pathway for its production exists in this organism. Indeed, the presence of PAF-AH activity in *S. cerevisiae* and *S. pombe* has been alluded to by mass spectrometry data (95). Also, *Ale1* the gene encoding L-PAF-AT has been found in yeast (83, 96, 97). All of these findings signify the presence of the remodelling pathway in yeast or part thereof.

Yeast does not have any recognizable PAF-receptor homolog yet was shown to be sensitive to PAF treatment (94). A BLAST search for the PAF-receptor against the yeast genome yields a partial but strong match with *SEC7* (92), which is part of the vesicle coat involved in trafficking and is thought to be a guanine nucleotide exchange factor. Further, the sensitivity to PAF was dose-dependant and was partially reversed by pre-treatment with a PAF antagonist which binds to the receptor in neurons by competing with PAF (94). However Sec7 is not localized to the plasma membrane (98), thus, the presence of the PAF-receptor in yeast remains questionable.

The sensitivity of yeast to PAF is enhanced upon deletion of three enzymes (*SPO14*, *SCT1*, and *GPT2*) belonging to the glycerophospholipid biosynthetic pathway, indicating that PAF is entering the cells upon treatment or eliciting intracellular changes in glycerophospholipid metabolism (99). Only three mutants were analyzed in that particular study and the complete PAF biosynthetic or remodelling pathways in yeast have yet to be elucidated. *Nor has a systematic genome-wide survey of deletion mutants hypersensitive to PAF treatment been conducted.*

In terms of yeast physiological changes upon PAF treatment, it was reported that membrane adenylate cyclase activity and cAMP levels decreased upon PAF treatment and this was partially reversed by pre-treatment with a PAF antagonist (94). Surprisingly, an increase in yeast PAF levels during mating was suggested to be stimulated by calcium influx caused by mating factor (94). Isolated yeast vacuoles treated with PAF showed stimulated vacuolar ATPase and pyrophosphatase activities leading to a lower proton potential on the vacuolar membranes and decreased calcium transport (100). This illustrates that PAF exists in yeast and that the pathways for its production likely exist. However, the role of PAF in yeast is not known.

1.7 Yeast As A Model For PAF Cytotoxicity

The goal of this study is to exploit chemical genomic screens in yeast to provide insight into how C16:0 PAF elicits neuronal cell death independent of its receptor. This approach was chosen because yeast likely do not have a recognizable PAF-receptor, are highly conserved with mammals, and have been successfully used to study amyloidoses. More importantly, yeast screens have been successfully employed to reveal the targets and metabolizing enzymes of similar phospholipids and lyso-phospholipids. Wildtype yeast as well as numerous mutants (genome wide in some cases) have been challenged with C16:0 PAF, C16:0 L-PAF, C16:0 lysophosphatidylcholine and edelfosine (a similar synthetic ether lipid) and their growth phenotype assessed (99, 101, 102). The mutants that were tested in these studies belonged to the glycerophospholipid biosynthetic pathway only. Importantly these studies determined that treating yeast with high levels of these lipids required to produce a cellular effect in yeast (μM range), produced distinct cellular effects on growth and lipid metabolism as opposed to a non-specific detergent

effect on the membrane. The hypersensitivity of *SPO14*, *SCT1*, and *GPT2* deletion mutant strains to PAF strongly suggests that, due to their predicted roles in PAF metabolism, screening genome-wide mutant arrays for PAF sensitivity is not only feasible, but will likely successfully isolate mutants specifically involved in cellular response to PAF.

Chemical-genomic screens in the case of lipid diseases, yeast, and an ether lipid (edelfosine) were used for the study of Niemann-Pick Type C (NP-C) disease and further argue that ether lipids can be studied using yeast. NP-C is an autosomal recessive neurodegenerative disorder affecting lipid metabolism and storage that causes accumulation of low-density lipoprotein derived cholesterol and tissue specific lysosomal accumulation of glycoproteins and phospholipids (103, 104). Mutations in NPC1 are found in the majority of Niemann-Pick disease type C (NP-C) patients. *NCR1* is the yeast homolog of NPC1 (105) and deletion of *NCR1* conferred resistance to the anti-tumor drug edelfosine. This increased resistance to edelfosine in the *ncr1Δ* strains was exploited for the study of mutations corresponding to those found in the NPC1 gene from patients with NP-C (105) stressing the power of this model system. Even though edelfosine is an ether lipid that was used at high levels above its critical micelle concentration, the yeast model did not exhibit non-specific detergent effects (105, 106) but rather showed specific differences between the *NCR1* mutants tested. Other edelfosine studies in yeast further indicate that ether lipid signalling can be examined using this system (99, 105-108). For example, an overexpression screen of yeast genes that cause growth defects upon treatment with edelfosine (108) did not identify cell wall or membrane proteins that would have been expected if the ether lipid was causing non-specific detergent effects

rather than a specific signalling response. In addition it was determined that edelfosine induces apoptosis via the same mechanism in yeast and in tumor cells (106) again highlighting the conservation and specificity.

Similar studies have also been conducted using C16:0 lysophosphatidylcholine (101). An overexpression screen, in which mutants express each gene in the genome on a plasmid, was used to observe the toxicity of C16:0 lysophosphatidylcholine. The screen uncovered a novel phospholipase B in yeast (101) and this emphasizes the relevance of this type of study of lipids in revealing mechanistic information. Interestingly, a fluorescently labelled phosphatidylcholine was observed inside the cells upon treatment indicating that exogenous treatment of lipids leads to their internalization (105) and that the cellular growth defects are not just due to plasma membrane effects.

All of these studies indicate that the signalling and cellular effects of ether lipids can be studied using yeast. Hence, I hypothesize that not only will high-throughput PAF yeast chemical genomic screens be feasible, but they will yield relevant and invaluable insight into the mechanism of PAF signalling and neuronal death.

1.8 Chemogenomics: A Systems Biology Approach For Drug Target Discovery

The emerging field of systems biology aims to understand complex biological phenomena not by using the reductionist approach but rather by observing all the components (and their relationships) in a system (109, 110). This is done by integration of computational and experimental tools (reviewed in 110, 111). Recently, this field has gained much popularity due to the emergence of high-throughput techniques (112) that generate data for a system and quickly allow for model creation (reviewed in 113, 114).

The systems biology approach is discovery-driven and is a multidisciplinary alternative to the classical molecular biology approach (115). In this project, I have employed a series of systems biology approaches available in yeast to predict the molecular mechanism or mode-of-action of C16:0 PAF. The techniques I employ are yeast chemical-genomic screens, synthetic-lethal synthetic genetic array (SL-SGA) screens, as well as mass spectrometry based lipidomics profiling. Below I review these techniques:

1.8.1 Deletion Mutant Arrays.

The ease of directed mutagenesis in yeast has lead to the production of several deletion mutant libraries that are used in both functional- and chemical- genomic studies. A kanamycin-resistance cassette having a unique bar-code (DNA sequence) was used to construct a haploid deletion mutant array consisting of 4000+ haploid yeast strains each missing one gene and a heterozygous deletion mutant array consisting of 6000+ diploid yeast strains (30). These deletion mutant libraries are the essential reagents for both chemical- and functional- genomic screening described below.

1.8.2 Yeast Chemical-Genomics

The deletion mutant arrays have been successfully exploited to help uncover the mode-of-action of many compounds (reviewed in 116). Two commonly used screens are known as chemogenomic (or chemical-genetic) profiling and drug-induced haploinsufficiency profiling. Chemogenomic screens use the haploid deletion mutant array (Figure 2) and are based on the principle that deleting a gene that normally protects yeast from the toxic effects of a drug should enhance the toxicity and uncover the target of the drug (117). A disadvantage of this haploid based screen is that only non-essential

Screen1: Chemical-Genetic Profiling

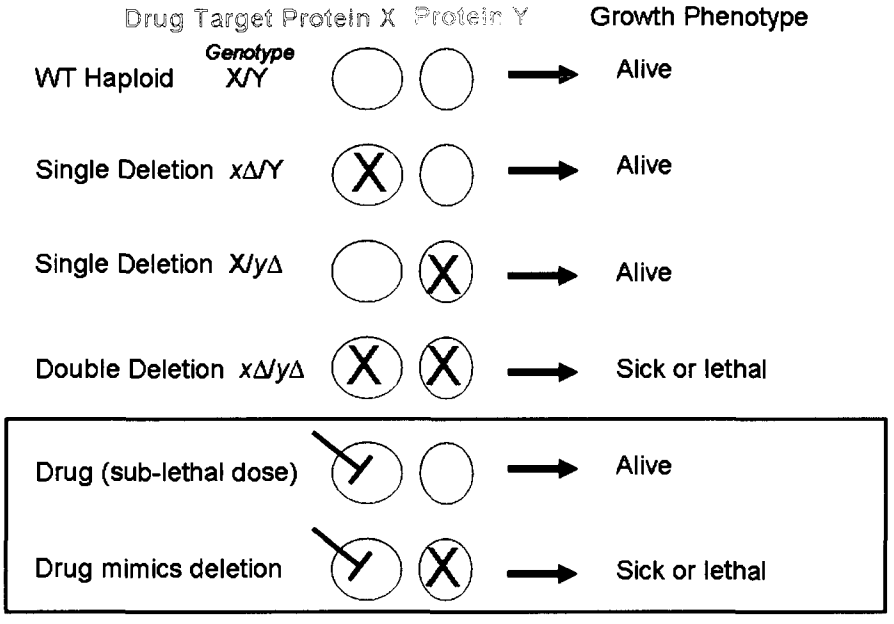

Figure 2. Schematic representation of Chemical-Genetic Profiling. A haploid mutant of a non-essential gene (represented by an *X*) is hypersensitive to sublethal concentrations of a drug (represented by a T) and is likely synthetically lethal with the target of the drug. Thus, chemical-genetic interactions identify drug targets via "guilt by association" such that a single deletion (protein *yΔ*) is alive but with drug treatment the phenotype mimics that of a double deletion (protein *yΔ* and drug target *xΔ*) – shown in the red box.

genes are assessed for sensitivity to the compound. This screen is then complemented with the heterozygous deletion mutant array chemical-genetic screen commonly known as Drug Induced Haploinsufficiency profiling (118, 119). The heterozygous diploid screen is based on the principle that reducing the copy number of the target of a drug in a diploid should increase the inhibition caused by semi-inhibitory concentrations of that compound (Figure 3). This screen does utilize essential genes and could potentially lead to the discovery of direct targets as opposed to the processes or parallel pathways identified by the haploid screen.

There are two commonly used methods for screening deletion mutant arrays for drug sensitivity. First, the growth of each deletion mutant strain can be directly monitored on agar plates containing the compound of interest (117). This direct-measurement of individual mutant growth can be easily facilitated through precise and reproducible robotic-based manipulation of the deletion mutant arrays and computer based scoring of colony growth. The growth of each mutant on control versus compound media is scored to identify mutants with enhanced toxicity. In a parallel method, all the deletion mutant cells can be pooled into one test tube such that each mutant is represented equally. This type of screen uses liquid media containing the compound to challenge the pooled mutants. The starting culture is thus treated equally and the relative growth of each mutant is monitored over time. Since all the mutants a mixed together, their relative growth is assessed using the built in bar-codes and DNA microarrays (119, 120).

1.8.3 Yeast Functional Genomics

Pathways and processes in yeast are sometimes redundant or parallel. This redundancy can make the assignment of biological function of genes a challenge as many

Screen2: Drug-Induced Haploinsufficiency Profiling

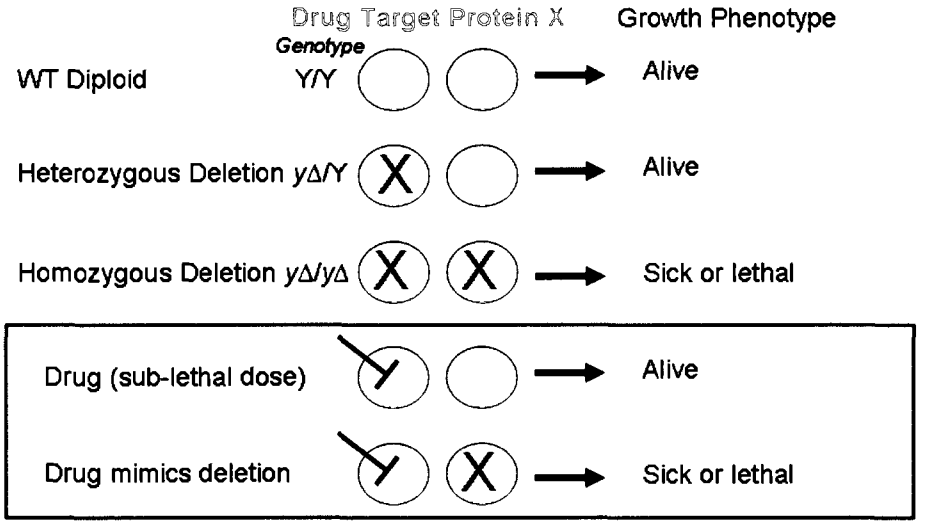

Figure 3. Schematic representation of Drug Induced Haploinsufficiency Profiling. In a diploid cell the target of a drug acting on a gene product can be uncovered by lowering the gene copy number from two copies to one resulting in hypersensitivity to that drug. The drug, even at semi-inhibitory levels, may become toxic when its target's copy number is reduced. A drug target (represented by a blue circle) is present in the cell at levels that keeps it resistant to sublethal concentrations of that drug (represented by a T). However, lowering the gene dosage of the target by 50% renders the cell hypersensitive to the drug and thus uncovers the target – shown in the red box.

deletion mutants display no observable phenotype because the remaining parallel pathway can compensate. In many cases, only when a single deletion is combined with a deletion of a gene in the parallel pathway does a phenotype arise. This has been termed synthetic lethality (SL) and occurs when the combined deletion of two non-essential genes in a haploid yeast cell results in slow growth or lethality as compared to each deletion on its own (Figure 4). SL interactions are able to predict the function of uncharacterized genes. For example, a gene with an unknown function may be linked to a pathway with a known function via synthetic lethality thus providing hints as to its own role in the cell. Synthetic Genetic Array (SGA) is a methodology that allows for systematic creation of double mutants in a genome-wide manner (Figure 5) (40). This tool utilizes the haploid deletion mutant array and through a process of mating and genetic selection produces a new array of double deletion mutants (the original non-essential gene deletion plus a secondary deletion of interest). The final double mutant array can be screened for virtually any phenotype of interest. The most common phenotype that is assessed is the growth or fitness defect compared to each of the single mutants. The power of this method comes in when a genome-wide SL interaction map is produced for a gene of interest as it allows for hypothesis generation with regards to every possible process that the gene may be involved in.

SL-SGA data can be integrated with chemical-genetic data in a manner that allows for prediction of the direct target of a drug. Synthetic lethality is based on parallel pathways while chemical-genetic screens are designed to uncover genes that when deleted exacerbate the effect of a drug. The drug may be acting on the pathway parallel to the deletion and would thus mimic a secondary deletion causing a synthetic chemical

Principle behind Synthetic Lethal interactions

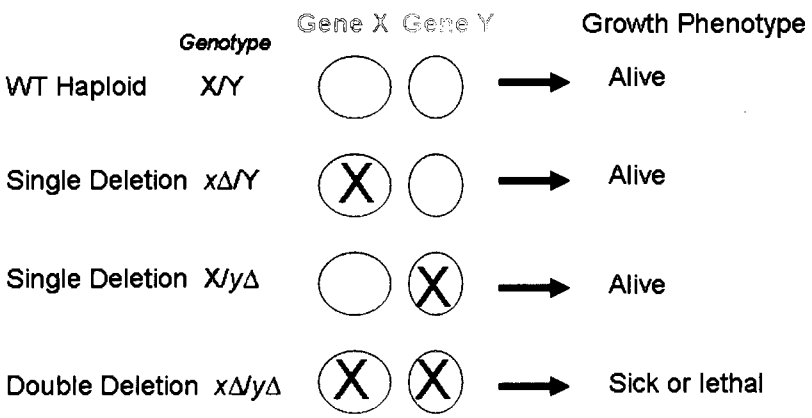

Figure 4. Schematic representation of Synthetic Genetic interactions. A synthetic sick or synthetic lethal (SL) interaction occurs when the combined deletion of two non-essential genes in a haploid yeast cell results in slow growth or lethality as compared to each deletion on its own.

interaction. For example, a haploid deletion mutant library was used for screening 12 compounds to find mutant enhancers of toxicity and this approach was integrated with synthetic lethal data to find the target pathways (117).

1.8.4 Lipidomics: Mass Spectrometric Profiling Of Phospholipids

Advances in mass spectrometry techniques have allowed for the high throughput analysis of complex mixtures of lipids (reviewed in 45). Lipidomics is defined as the systems-level cataloguing of lipid species and their associated factors and proteins for the purpose of drug and biomarker discovery. The identification and quantitation of lipids extracted from biological samples is a hallmark of lipidomics. The principle behind this technique is that lipids are extracted by conventional methods and analyzed on a mass spectrometer such that the fragmentation patterns offer insight into the structure of the molecules. Advances in ionization methods have allowed for greater precision in lipid structure identification. In this study, phosphocholine containing lipids are identified by their fragmentation pattern since they produce a phosphocholine fragment having a known mass-to-charge ratio. This method allows for a semi-global search for changes in phosphocholine-containing lipid profiles of biological samples. For example, this technique was used to compare phosphocholine-containing lipids such as PAF in neuronal cell lines before and after differentiation (121). In this project, I have utilized this technique with help from collaborators to address certain questions that would aid in the interpretation of the chemical-genomic screening results.

Synthetic Genetic Array (SGA) screening

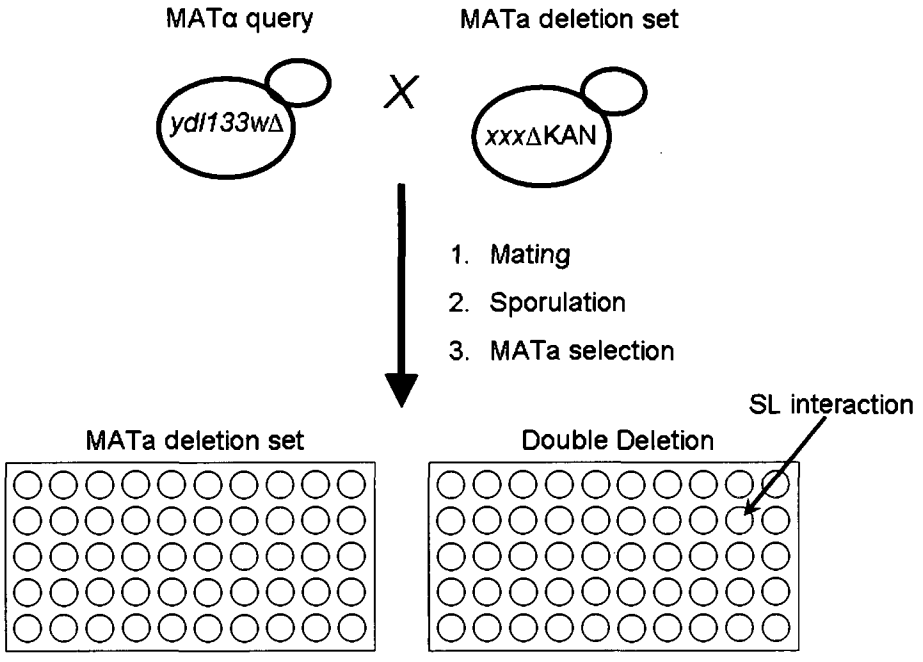

Figure 5. Schematic representation of Synthetic Genetic Array (SGA) screening. An SGA screen allows for identification of genome-wide SL and SS interactions for a particular gene of interest by creating double mutants in a haploid yeast cell. In the case of this study, a *MATα ydl133wΔ* query strain is mated to the *MATa* deletion mutant array. After sporulation, haploid selection, and double mutant selection via a series of replica pinning and genetic selection steps, the resulting array of double mutants is evaluated for the presence of SL or SS interactions.

1.9 Hypothesis

While most studies on PAF signalling have been performed in mammalian systems, to date, very little work has been done using lower eukaryotes such as yeast as model systems for PAF studies. Studies performed on other compounds, including lipids, using yeast chemical-genomic techniques have been successful at revealing target pathways or mode-of-action. To gain further insight into receptor-independent PAF neuronal toxicity I used yeast chemical genomics to test the hypothesis that *PAF is cytotoxic to yeast and acts through multiple cellular pathways in the cell that parallel those found in mammals.*

Towards this end, I had three specific aims. 1) Characterize the sensitivity of yeast to PAF by examining its growth, cell cycle progression, and viability upon PAF challenge. 2) To perform and confirm yeast genome-wide chemical-genetic profiling and genome-wide drug-induced haploid insufficiency screens for C16:0 PAF and C16:0 L-PAF using the yeast haploid deletion mutant array and the yeast diploid heterozygous deletion mutant array, respectively. 3) Use the chemical-genomic profiles for PAF and L-PAF make testable hypotheses with regards to the mode-of-action. This work provides novel insight into the molecular mechanism of PAF signalling and influences our understanding of Alzheimer's disease progression.

CHAPTER 2: MATERIALS AND METHODS

This section outlines reagents, solutions, and buffers used including their source as well as which strains were used and the protocol for each experiment.

2.1 Reagents

Both C16:0 PAF and C16:0 L-PAF were purchased from Cedarlane Laboratories Limited, Ontario, Canada. YPD consisted of 1% yeast extract, 2% peptone, 2% glucose. Yeast Extract was purchased from Wisent Bioproducts, Quebec, Canada. Bacto Peptone was purchased from BD biosciences, Mississauga, Canada. Note that Bacto Peptone from Wisent Bioproducts exhibited an interaction with C16:0 PAF that gave non-specific results so it was avoided. DAPI (D1306), Rhodamine phalloidin (R415), and goat anti-mouse IgG with Alexa Fluor 488 (MP 00852) were purchased from Invitrogen. Antibodies for GFP were from Santa Cruz Biotechnology (SC-8334), and Anti-c-Myc Mouse monoclonal antibody (clone 9E10) from Roche. Clonat was purchased from Werner (Cat#5.5OOO), L-Canavanine from sigma (Cat#C9758-5G), and G418 from Wisent (Cat#400-130-QG).

Strains used in this study

Strain	Other name	Genotype
YKB779	YPH499	*MATa ade2-101, his3-Δ200, lys2-801, leu2-Δ1, ura3-52, trp1-Δ63*
YKB780	YPH500	*MATα ade2-101, his3-Δ200, lys2-801, leu2-Δ1, ura3-52, trp1-Δ63*
YKB1079	BY4741	*MATa his3Δ1, leu2Δ0, met15Δ0, ura3Δ0*
YKB1118	BY4742	*MATα his3Δ1, leu2Δ0, lys2Δ0, ura3Δ0*
YKB1117	BY4743	*MATa/α his3Δ1, leu2Δ0, lys2Δ0, ura3Δ0*
YKB1140		*MATa/α ade2-101, his3-Δ200, lys2-801, leu2-Δ1, ura3-52, trp1-Δ63*
YKB1203		*MATα ade2-101, his3-Δ200, lys2-801, leu2-Δ1, ura3-52, trp1-Δ63, YDL133w-GFP::KanMX*
YKB1191		*MATa ade2-101, his3-Δ200, lys2-801, leu2-Δ1, trp1-Δ63, ura3Δ::Tub1p-GFP-Tub1*
YKB1164		*MATα ade2-101, his3-Δ200, lys2-801, leu2-Δ1, ura3-52 trp1-Δ63, ydl133wΔ::KanMX*
YKB1206		*MATa ade2-101, his3-Δ200, lys2-801, leu2-Δ1, ura3-52, trp1-Δ63, ccs1Δ::KanMX*
YKB1185		*MATα can1Δ::STE2pr-Sp-his5, lyp1Δ, his3Δ1, leu2Δ0, ura3Δ0, met15Δ0, LYS2, ydl133wΔ::natMX4*

2.2 Chemical-Genetic Profiling

The *MATa* haploid deletion mutants were purchased from Open Biosystems (Cat# YSC1053) (30). Strains were robotically pinned in duplicate onto YPD + 200mg/L G418 (2% peptone, 1% yeast extract, 2% glucose, 2% Agar) plates at a density of 1536 colonies per plate using the Singer Rotor HDA and grown for 3 days at 25°C. These plates were pinned onto YPD containing either Ethanol, 120μM PAF, or 120μM L-PAF. Plates were incubated at 25°C and pictures taken using a Biorad Imager at 15 and 40 hours. The sensitivity of each mutant was assessed visually by comparing colony sizes on the treated plates to the ethanol control plates. To supplement the visual scoring and reduce false negatives I also employed a computer-based scoring method. Tiff images of the plates were used to quantify pixel intensity, and thus colony size, using commercially available AlphaEaseFC V4.0.0 from Alpha Innotech Corporation, California, USA.

Colonies on each plate were normalized to their plate's average and compared to their respective ethanol treated colonies as described (122). The screen was performed in triplicate and any interactions identified at least 2 out of 3 times for each compound were confirmed by quantitative growth curves. To increase the number of putative hits and increase the chances of finding more interactions, I also confirmed by growth curves the interactions that appeared at least once for both compounds. I removed multiple-drug resistance (MDR) genes based on published literature (117, 120).

2.3 Growth Curves

Yeast cultures were inoculated into 5mLs of YPD and grown overnight at 25°C in a roller drum. Next morning (~18 hours later), OD_{600} was measured and strains were diluted to OD_{600} = 0.2 in 5mL YPD. This pre-growth was done for 4 hours to get cells into log phase. The final OD_{600} was measured and a 2X stock of cells was made (OD_{600} = 0.1). 96-wells were inoculated using 100μL of 2X stock of cells and 100μL YPD containing ethanol, Ethanol, PAF, or L-PAF at 2X the desired final concentration. Each strain was inoculated in triplicate. The plate was immediately taken to the plate-reader (Multiskan Ascent, Thermo Labsystems) to be shaken at 960rpm and measured 45 times at 25minutesintervals. Temperature was maintained at 25°C. Shaking was not continuous and the protocol consisted of 20minuteswaiting then Shaking at 960rpm for 5minutesthen measuring. Fold decrease in area under the curve for each mutant compared to Wildtype (WT) on that day was calculated by the formula: [(Area Treated / Area Control)$_{WT}$ / (Area Treated / Area Control)$_{MUTANT}$].

2.4 Drug-Induced Haploinsufficiency Screen

The heterozygous diploid deletion mutants were purchased from Open Biosystems (Cat# YSC1055). Strains were robotically pinned in duplicate onto YPD + 200mg/L G418 (2% peptone, 1% yeast extract, 2% glucose, 2% Agar) plates at a density of 1536 colonies per plate using the Singer Rotor HDA and grown for 3 days at 25°C. These plates were pinned onto YPD containing either 2.4% Ethanol, 240μM PAF, or 240μM L-PAF. Plates were incubated at 25°C and pictures taken using a Biorad Imager at 12, 20, 45 and 72 hours. The sensitivity of each mutant was assessed visually by comparing colony sizes on the treated plates to the ethanol control plates. To supplement the visual scoring and reduce false negatives I also employed a computer-based scoring method. Tiff images of the plates were used to quantify pixel intensity, and thus colony size, using commercially available AlphaEaseFC V4.0.0 from Alpha Innotech Corporation, California, USA. Colonies on each plate were normalized to their plate's average and compared to their respective ethanol treated colonies. The screen was performed in duplicate and any putative hits confirmed by quantitative growth curves.

2.5 Lipidomics Profiling

I) pre-growth and treatments:

Using the haploid yeast wildtype strain (BY4741), 5mL YPD (glass tube) was inoculated and incubated overnight at 25°C in a rotating drum. Next morning, the OD_{600} was measured and the cells diluted to OD_{600} = 0.2 in 5mL YPD and incubated at 25°C for 4 hours in a rotating drum. Using 15ml plastic tubes, nine samples were prepared and treated with Ethanol, PAF, or L-PAF as indicated in the table below such that the final volume was 1mL. The samples were vortexed 3 times to mix and incubated at 25°C for

13.75 hours in a rotating drum. Samples A-F were centrifuged for 2minutesat 3000 RPM, at 4°C. Samples G, H, and I were placed on ice for a few minutes to be used for OD_{600} measurement and for counting final cell density using a hemacytometer. Samples A, C, and E had cell pellets so the supernatant was removed to new tubes. 1mL of ice-cold acidified methanol [acidified with 2% acetic acid] was added to each sample and the cell pellets, if any, were resuspended immediately to prevent clumping. The samples were then kept on ice and transferred to the Bennett Lab for lipid extraction.

List of samples prepared after the 4hour pre-growth

A)	YPD+cells at OD_{600} Initial = 0.05 + 40μM PAF [ie 4μl of 10mM Stock]
B)	YPD no cells + 40μM PAF
C)	YPD+cells at OD_{600} Initial = 0.05 + 40μM *L*-PAF
D)	YPD no cells + 40μM *L*-PAF
E)	YPD+cells at OD_{600} Initial = 0.05 + 4μL Ethanol
F)	YPD + 4μL Ethanol treatment
G)	YPD+cells at OD_{600} Initial = 0.05 + 40μM PAF [for counting cells]
H)	YPD+cells at OD_{600} Initial = 0.05 + 40μM *L*-PAF [for counting cells]
I)	YPD+cells at OD_{600} Initial = 0.05 + 4μL Ethanol [for counting cells]

II) Lipid extractions:

In order to extract glycerophospholipids I used a modified Bligh and Dyer method (121, 123, 124). Samples were on ice in 1mL acidified methanol (2% acetic acid) as mentioned above. 41.3μL of a 10uM stock of C13 LPC was spiked prior to extraction to control for extraction efficiencies and the lipids were extracted using a volumetric ratio of 0.95 and 0.8 of chloroform and NaAcetate 0.1M (aq) respectively, per volume of methanol in acid-washed borosilicate glass tubes (Fisher, Ottawa, ON, Canada). For my samples, this was 4mL acidified methanol (1mL from sample plus 3mL added), 3.8mL chloroform, and 3.2mL 0.1M NaAcetate. The organic phase was collected after centrifugation while the aqueous layer was back-extracted three times using a wash solution. The wash solution

contained 1.6mL YPD media, 4mL methanol (not acidified), 6mL chloroform, and 1.6mL NaAcetate (corresponds to the volumetric ratio of 1:2.5:3.75:1). The wash solution did not contain BSA. The organic fractions were pooled and evaporated under a stream of nitrogen gas to be dissolved in 300μL of ethanol and stored at -80°C in plastic eppitubes. (The amount of C13 LPC standard corresponds to 187.5ng in the 300μL ethanol at the end of the extraction. Which means that 5ng will be in the 8μL that are run on the Mass Spectrometer.) Analytes were introduced into a 2000 Q TRAP mass spectrometer via a microflow 1100 HPLC system (Agilent, Palo Alto, CA). The Q TRAP was operated with Analyst 1.4.1 (Applied Biosystems/MDS Sciex, Concord, ON, Canada). Details of the parameters were as published (121).

II) Data analysis and lipid profiling.

Using the Analyst software, lipid profiling was performed as follows. For each sample file, the precursor ion scan was plotted as Intensity (cps) vs. m/z (amu). The m/z was acquired using the range of 450-600. The extracted ion chromatograph (XIC) for each species of interest was plotted using the range N-1 to N+1.5, N being the peak m/z for that species. XICs for each species indicate its retention time (RT) and aid in species identification as well as quantification of the area under that peak. The area for the C13:0 LPC internal standard was also determined and all other species areas were divided by that value for that sample. This would be the normalized value and the fold change would be the ratio of the normalized value from one sample to another for that species.

2.6 Yeast Transformation

PCR mediated transformation of yeast strains with the desired markers was done using established PCR methods (125) and by the Lithium Acetate transformation method (126). Successful transformation was confirmed by PCR.

2.7 F-Actin Staining And Fluorescent Microscopy

F-Actin staining protocols were based on established methods (127, 128). Overnight cultures of wildtype yeast (YKB779) were seeded in 50mL YPD at a starting OD_{600} = 0.4 and incubated at 30°C for 4 hours with shaking at 250rpm in an orbital shaker. When the OD_{600} reached 0.7, 5mL samples of OD_{600} = 0.3 were treated either Ethanol, 180μM C16:0 PAF, or 180μM C16:0 L-PAF for 4 hours while incubating at 25°C in a roller drum. The final OD_{600} was determined and the cells fixed for 10 minutes by adding formaldehyde to the media to a final concentration of 4%. The cells were then pelleted by centrifugation (3000rpm, 5 min) and fixed for 1 hour in PBS containing 4% formaldehyde at room temperature. The cells were washed twice with 1mL PBS and resuspended in 100μL PBS. 10μL of rhodamine phalloidin (6.6μM in MeOH) were added to the 100μL of fixed sample and it was stained in the dark for 1 hour. The cells were then pelleted by centrifugation (3000rpm, 3 min) and washed 5 times with 1mL PBS. Samples were resuspended in 50μL PBS and stored at 4°C for microscopy. 5μL of stained sample was resuspended in a drop of mounting media containing DAPI (50mg p-phenylenediamine (Sigma in 5mL 1X PBS; adjust to pH 9.0 (NaOH) add 45mL glycerol and stir to homogeneity. Add 2.25 μl 1mg/ml DAPI. Store at -70°C in the dark (aliquote in 1mL/eppendorf)). Clean slides were loaded with 1μL of cells in mounting media and a cover slip placed on top. Slides were viewed at 63X oil immersion objectives on a Leica

Microsystems DMI 6000B fluorescent microscope equipped with a digital CCD camera (C4742-80-12A6 Hamamatsu Photonics) under the control of the Volocity Software from Improvision. Image stacks with 0.3μm spacing were acquired for a total thickness of 5μm. On average, 65 cells were counted for the actin experiments. For the DAPI experiments, 97 cells were counted for PAF treatment, 55 for ethanol, and 89 L-PAF.

2.8 Spindle Tagging And Fluorescent Microscopy

A GFP tagged *TUB1* construct was integrated into the *URA3* locus of wildtype yeast (YKB1191). Overnight cultures (YKB1191) were grown in triplicate (3 different isolates). The samples were seeded in 5mL YPD at a starting OD_{600} = 0.2 and incubated at 25°C for 4 hours in a roller drum. When the OD_{600} reached 0.6, 2mL samples of OD_{600} = 0.05 were treated either Ethanol, 180μM C16:0 PAF, or 180μM C16:0 L-PAF for 3 hours while incubating at 25°C in a roller drum. The final OD_{600} was determined and the cells fixed for 10 minutes by adding formaldehyde to the media to a final concentration of 4%. The cells were then pelleted by centrifugation (3000rpm, 5 min) and fixed for 1 hour in PBS containing 4% formaldehyde at room temperature. The cells were washed twice with 1mL PBS and resuspended in 50μL PBS. 5μL of sample was resuspended in a drop of mounting media containing DAPI. Clean slides were loaded with 1μl of cells in mounting media and a cover slip placed on top. Slides were viewed at 63X oil immersion objectives on a Leica Microsystems DMI 6000B fluorescent microscope equipped with a digital CCD camera (C4742-80-12A6 Hamamatsu Photonics) under the control of the Volocity Software from Improvision. Images stacks with 0.7μm spacing were acquired for a total thickness of 5μm. On average, 88 cells were counted and the experiment done in Triplicate.

2.9 Yeast Immunofluorescence

Cells were grown to mid-log phase in 5mL YPD and fixed in 3.7% formaldehyde for 1hour followed by one wash in 0.1M potassium phosphate (pH7.5). Samples were resuspended in 1mL of "digestion buffer" (50 units/ml lyticase in 0.1M potassium phosphate (pH7.5) with 2μl/ml 2-β-mercaptoethanol) and incubated up to 30 minutes such that cells are spheroplasted and turn dark grey. Cells were pelleted at 2500rpm for 5minutesand washed three times with PBS to be resuspended in a final 1mL PBS. Poly-L-lysine coated 12-well slides were prepared and 10μL of cells placed on each well for a few minutes then aspirated off and the wells washed 3 times with PBS. The slides were immersed in cold methanol for 6 minutes and then cold acetone for 30 seconds then rehydrated with PBS. 15μL of blocking solution (PBS + 3%BSA) was placed on each well for incubation in a humid chamber for 30 minutes. After removing the blocking solution, 10μL of varying concentrations (1-10μg/ml) of primary antibody (anti-c-Myc) were placed on each well and incubated for 1 hour. Wells were then washed three times with blocking solution for secondary antibody treatment in the dark for 1 hour (CAT#A11017, Invitrogen). Wells were washed three times with blocking solution and a drop of mounting medium containing DAPI was placed on each well. Finally, a glass coverslip was placed on the slide and sealed with nail polish.

2.10 Immunoblotting

Whole Cell Extracts (WCE) were prepared from 30mL of cells from an overnight culture grown in YPD at 30°C. Cells were pelleted by centrifugation for washing with cold 1mL lysis buffer (20 mM HEPES, pH 7.4, 0.1% Tween 20, 2 mM $MgCl_2$, 300 mM NaCl). In a 1.5mL Eppendorf tube the cells were resuspended in 300μL lysis buffer and

an equal volume of acid-washed glass beads (Cat#35-535, Fisher Scientific). Samples were vortexed six times for 1minuteseach and placed on ice in between iterations of vortexing such that ~80% lysis was achieved. The WCE was isolated by centrifugation at 13,200rpm for 15minutesand samples frozen at -80°C. 2X loading buffer (100mM Tris, pH 6.8, 4% sodium dodecyl sulfate [SDS], 0.2% bromophenol blue, 20% glycerol, 200mM 2-β-mercaptoethanol) was used with an equal volume of WCE to boil the sample for 5 min. Proteins were separated by 7.5-10% SDS-polyacrylamide gel electrophoresis (PAGE). Standard Western blotting procedures were performed using the following antibodies: anti-c-Myc (Cat#11667149; Roche), peroxidase-conjugated goat anti-rabbit IgG (Cat#AP307P; Chemicon), peroxidase-conjugated goat anti-mouse IgG (Cat#170-6516; Bio-Rad), and anti-GFP (SC-8334, Santa Cruz Biotechnology). Electrophoretic transfer was done on nitrocellulose membranes using a semi-dry transfer apparatus (BioRad). The membranes were blocked in Phosphate-buffered saline (PBS) containing 5% nonfat dry milk and 0.1% Tween 20 (PBS-T), at 4°C overnight with gentle shaking. Primary and secondary antibody staining was 1hour each with 3X10minuteswashes with PBS-T in between. Gels were developed using the Immobilon Western chemiluminescent HRP substrate (Cat#WBKLS0500, Millipore) and a Biorad ChemiDoc XRS imager controlled by the Quantity One 4.6.1 software.

2.11 Determination Of Budding Index

Wildtype yeast (YKB779) were grown overnight in triplicate and seeded to an OD_{600} = 0.2 in 5mL then incubated at 25°C for 4 hours until the final OD_{600} = 0.7. Then, 5mL cultures at OD_{600} = 0.05 were treated with Ethanol, 180μM C16:0 PAF, or 180μM C16:0 L-PAF for 4 hours at 25°C in a roller drum. The final OD_{600} was determined and

the cells fixed for 10 minutes by adding formaldehyde to the media to a final concentration of 4%. The cells were then pelleted by centrifugation (3000rpm, 5 min) and fixed for 1 hour in PBS containing 4% formaldehyde at room temperature. The cells were washed twice with 1mL PBS and resuspended in 50μL PBS. Finally, samples were examined under a light microscope and the budding index determined by the fraction of budded cells (those not in G1) as calculated by this ratio: N_{budded}/N_{total}, where N is the number of cells. 200 cells were counted as in established protocols (129).

2.12 Determination Of Cell Viability By Colony Forming Units (CFU)

CFU counting was performed as described (105, 108). Triplicate overnight cultures of wildtype (YKB779) were seeded to an OD_{600} = 0.2 in 5mL of YPD and incubated at 25°C for 3 hours. Then, samples were diluted to OD_{600} = 0.05 in 5mL and treated with Ethanol, 180μM C16:0 PAF, or 180μM C16:0 L-PAF for 6 hours at 25°C in a roller drum. 10μl of sample was used for hemacytometer counting to determine concentration (cells per μl). After appropriate dilution in YPD, 300cells were plated on YPD plates and spread by glass beads. Colonies were counted after 2days incubation at 30°C and percent viability was calculated by setting the number of colonies formed in Ethanol treated samples to 100%.

2.13 SL-SGA Of *YDL133w*

The ***MATa*** deletion mutant library was acquired from Open Biosystems (CAT# YSC1053). A ***MATα*** query strain containing a *ydl133wΔ::NatMX4* (YKB1185) was constructed as described in "transformation" above. A Singer RoToR HDA (Singer Instruments) was used to manipulate the deletion library and the genome-wide SL-SGA

screen was performed according to established protocols (40). All steps were carried out in triplicate at 30°C except for sporulation (room temperature). The sensitivity of each mutant was assessed visually by examining colony sizes. To supplement the visual scoring and reduce false negatives I also employed a computer-based scoring method. Tiff images of the plates were used to quantify pixel intensity, and thus colony size, using commercially available AlphaEaseFC V4.0.0 from Alpha Innotech Corporation, California, USA. Colonies on each plate were normalized to their plate's average and compared to their respective control colonies as described (122). In this way, a list of putative hits was generated and ranked based on number of times a hit was observed out of three times and also based on the strength of the interaction. This putative list was confirmed by tetrad dissection on YPD plates at 30°C.

CHAPTER 3: RESULTS

3.1 Yeast Dose-Dependant Sensitivity To C16:0 PAF

It has previously been demonstrated that *S. cerevisiae* growth was inhibited upon treatment with C16:0 PAF (94). In order to confirm the sensitivity and identify semi-inhibitory concentrations of C16:0 PAF I performed automated growth curve analysis. In addition, as C16:0 L-PAF does not illicit neuronal cell death (11, 60) I also performed growth curve analysis using C16:0 L-PAF as a negative control. Growth curve analysis allows for quantitative, as well as visual, assessment of growth rate in comparison to control treatment. I found that wildtype yeast cells are sensitive to C16:0 PAF in a dose-dependent manner with dramatic inhibition at 180μM (Figure 6a). In contrast, equivalent concentrations of C16:0 L-PAF do not inhibit growth to the same extent (Figure 6b). These results suggest that similar to neuronal cells, yeast are sensitive to C16:0 PAF but not L-PAF and suggest that yeast have at least one C16:0 PAF target. The similarity in C16:0 PAF sensitivity between man and yeast suggest that despite the dramatic differences between yeast and neuronal cells, yeast may contain conserved biological processes and pathways impacted by PAF that maybe identified via chemical-genetic methods.

A

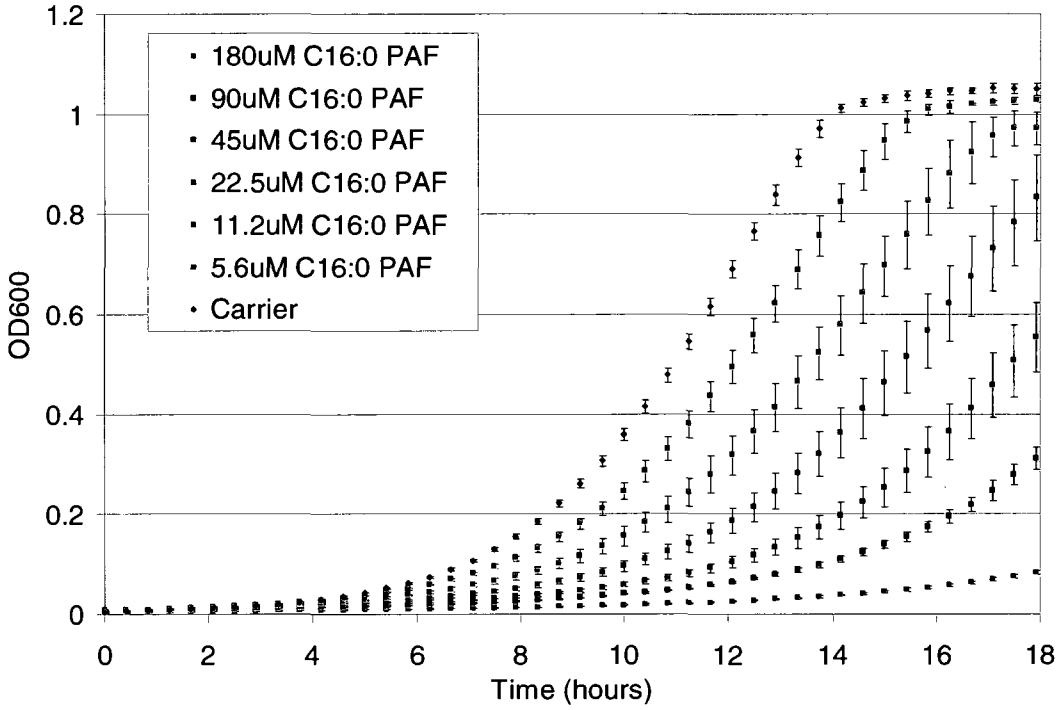
180uM C16:0 PAF
90uM C16:0 PAF
45uM C16:0 PAF
22.5uM C16:0 PAF
11.2uM C16:0 PAF
5.6uM C16:0 PAF
Carrier
OD600
Time (hours)
0
0.2
0.4
0.6
0.8
1
1.2
0
2
4
6
8
10
12
14
16
18

B

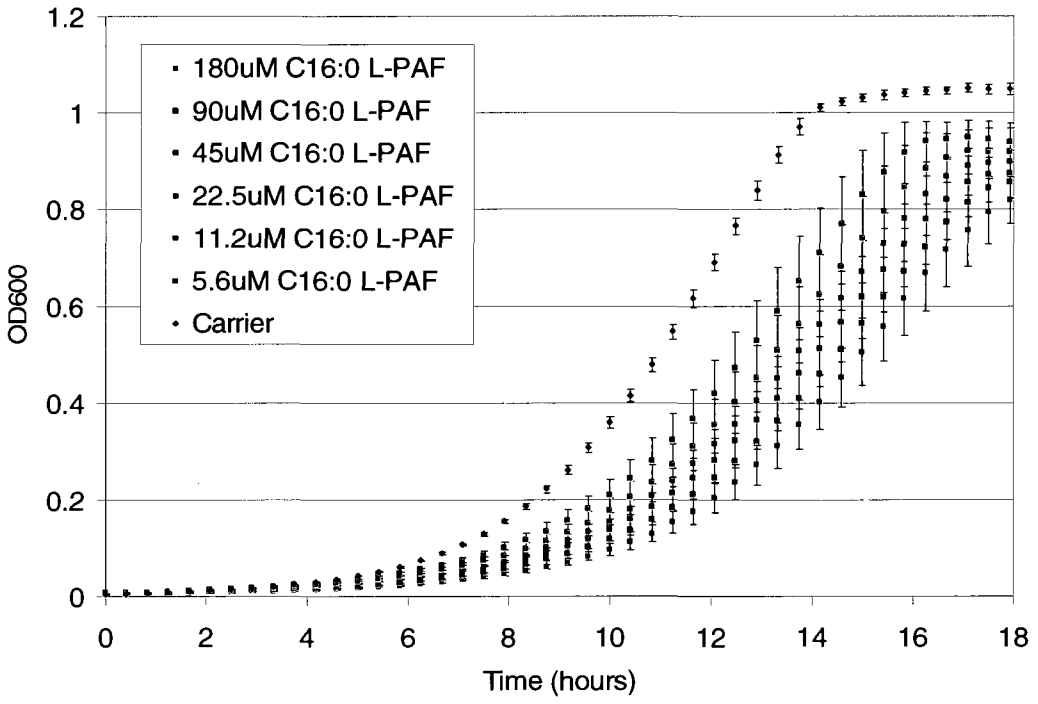
180uM C16:0 L-PAF
90uM C16:0 L-PAF
45uM C16:0 L-PAF
22.5uM C16:0 L-PAF
11.2uM C16:0 L-PAF
5.6uM C16:0 L-PAF
Carrier
OD600
Time (hours)
0
0.2
0.4
0.6
0.8
1
1.2
0
2
4
6
8
10
12
14
16
18

Figure 6. C16:0 PAF affects wildtype yeast proliferation in a dose-dependant manner. Automated yeast growth curve of *MAT*a wildtype strain (YKB779) showing OD_{600} as a function of time in hours. Triplicate cultures were grown in YPD (1% yeast extract, 2% peptone, 2% glucose) at 25°C and treated with ethanol carrier or varying concentrations of C16:0 PAF (Panel A) or L-PAF (Panel B). OD_{600} measurements of the samples were taken every 25 minutes in a plate-reader (Multiskan Ascent, Thermo Labsystems). Error bars represent one Standard deviation.

3.2 Yeast Has A Lower Budding Index Upon C16:0 PAF Challenge

C16:0 PAF levels in both mammalian and yeast systems seem to be cell cycle dependant (67, 93), hence I was interested in determining whether C16:0 PAF treatment causes a specific cell cycle arrest or delay. To test this, I examined budding index of wildtype yeast cultures treated with ethanol carrier control, 180μM C16:0 L-PAF, or C16:0 PAF. This concentration of C16:0 PAF showed the greatest inhibition of growth (Figure 6) and was thus chosen for this experiment. In yeast, the size of the bud is indicative of the position of the cell in the cell cycle with, with G1 cells having no buds, S-phase cells having small bud, and G2/M cells having a large bud. Budding index, the ratio of budded cells to the total number of cells, of logarithmically growing wildtype yeast is usually 75%. Similar to other studies on wildtype cells (129), I observed that wildtype cells treated with either ethanol and L-PAF had the expected budding index of ~75% while the PAF treated cultures exhibited a significant decrease in budding index (Figure 7). This suggests that PAF treatment impinges on cell cycle progression in yeast and causes cells to have a mild delay or arrest in G1.

3.3 C16:0 PAF Is Cytotoxic To Yeast Cells

The mild G1 accumulation of cells upon treatment with 180μM C16:0 PAF suggests that the dramatic growth defects displayed at this concentration of C16:0 PAF is likely not due to cell cycle arrest. To further characterize how the drug affects yeast, I performed a viability assay to determine whether yeast treated with C16:0 PAF for a period of 6 hours were able to form viable colonies after removal of the compound. If a

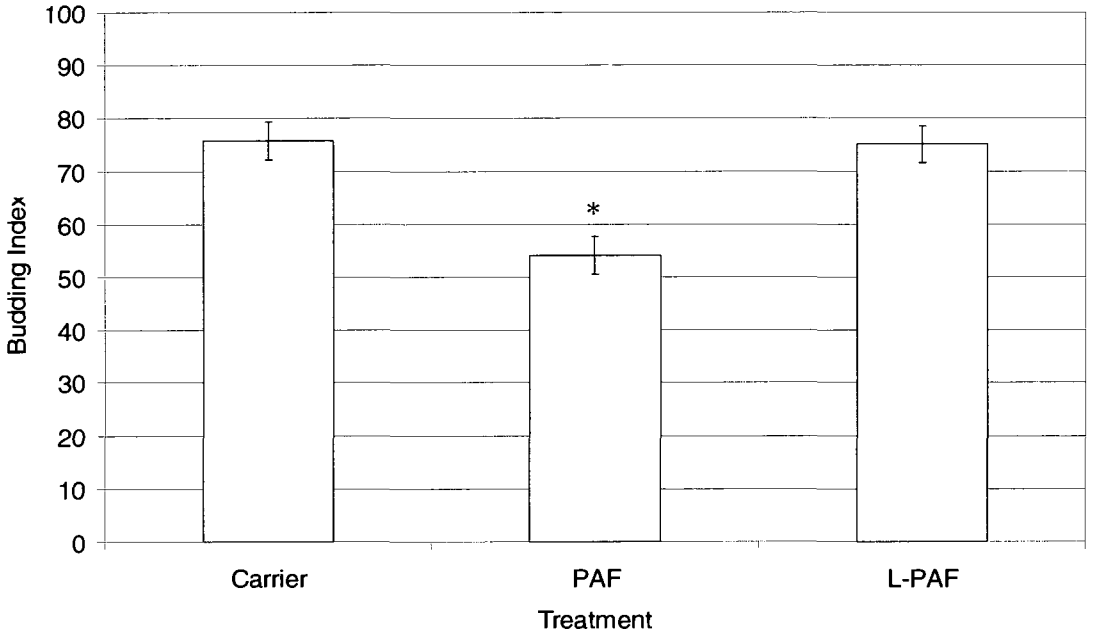
100
90
80
70
60
50
40
30
20
10
0
Budding Index
*
Carrier
PAF
L-PAF
Treatment

Figure 7. Budding index of wildtype yeast is lower upon treatment with 180μM C16:0 PAF but not L-PAF. Budding index of wildtype (YKB779) after 4 hours of treatment at 25°C with carrier, 180μM C16:0 PAF, or 180μM C16:0 L-PAF. Budding index is defined as the fraction of budded cells (those not in G1) in a yeast culture as calculated by this ratio: N_{budded}/N_{total}, where N is the number of cells. For each of the replicate experiments, 200 cells were counted (Wildtype n = 3, PAF and L-PAF n = 4). Error bars indicate one standard deviation. (* p-value < 0.05 for ANOVA, post hoc bonferroni correction one-tail t-test at Alpha = 0.05/3).

compound is cytostatic, treatment of the cells with the compound will inhibit growth, but upon its removal cells should remain viable and colonies should be formed. On the other hand, if a compound is cytotoxic, upon its removal cells will be inviable and unable to form colonies. In this way the ability of cells to form colonies after treatment indicates whether C16:0 PAF or L-PAF inhibit yeast growth (cytostatic effect) or whether they kill the cells (cytotoxic effect). Wildtype cells were incubated with ethanol carrier, 180μM L-PAF or 180μM C16:0 PAF for six hours and I asked if colonies could be formed on rich media plates after treatment. It was observed that 180μM C16:0 PAF but not L-PAF caused a significant decrease in viable cells after six hours of treatment indicating that it is cytotoxic to yeast at this concentration (Figure 8).

3.4 Chemogenomic Screens Of PAF Implicate It In Many Processes

The automated growth curves, budding index and cell viability assays indicated that at least one target for C16:0 PAF exists in yeast. Genome-wide yeast chemogenomic screens have been shown to be powerful tools for elucidating drug mode-of-action (120, 130, 131). Therefore, in an attempt to define the target(s) of C16:0 PAF and/or its signalling pathway(s) I embarked on screening for deletion mutants with enhanced sensitivity to C16:0 PAF, but not L-PAF. C16:0 L-PAF served as a good control because not only does it not elicit neuronal cell death (60) but also it is a lipid with almost the same structure as C16:0 PAF such that it can account for non-specific lipid effects. PAF and L-PAF were subjected to two complementary genome-wide screens: chemical-genetic profiling (Figure 2) using a haploid mutant library and drug induced haploinsufficiency profiling (Figure 3) using a heterozygous diploid mutant library. The first screen was performed in triplicate and 126 deletion mutants were putatively

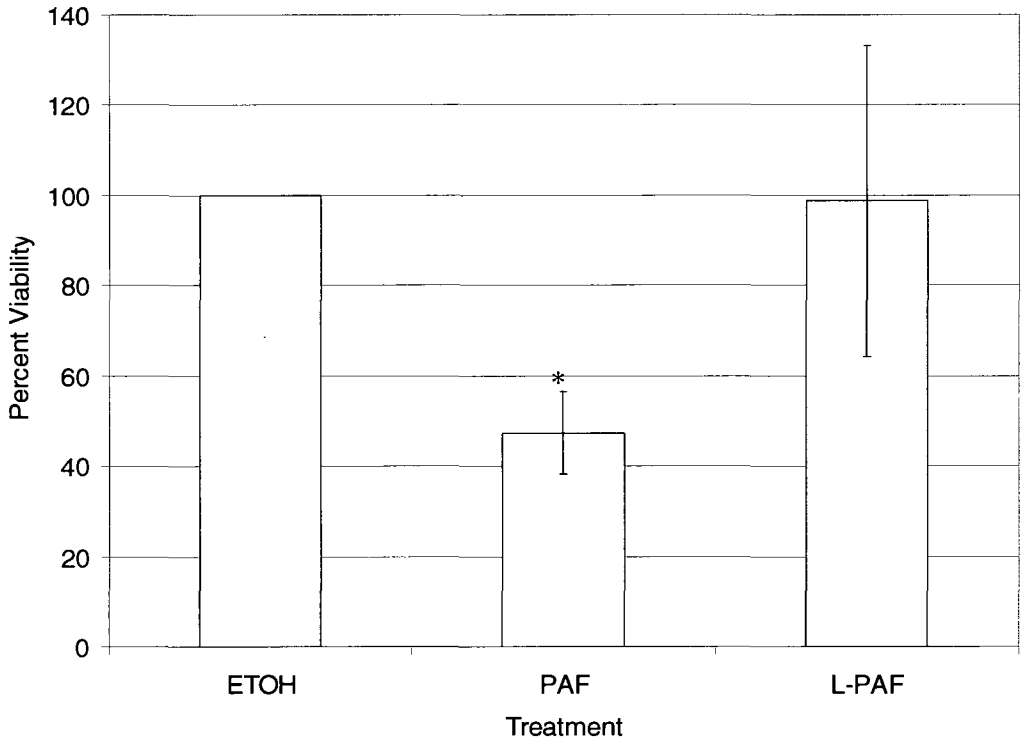
140
120
100
80
60
40
20
0
Percent Viability
*
ETOH
PAF
L-PAF
Treatment

Figure 8. 180μM C16:0 PAF is cytotoxic. Wildtype yeast cells (YKB779) were treated with Ethanol carrier, 180μM C16:0 PAF or 180μM L-PAF for 6 hours and subsequently 300 cells of each culture were seeded on YPD plates. Cell viability was determined by counting colonies formed on YPD after 2 days incubation at 30°C. The experiment was performed in triplicate. Percent viability was calculated by setting the number of colonies formed in Ethanol treated samples to 100%. Error bars represent one standard deviation. (* p-value < 0.05 ANOVA, post hoc bonferroni correction one-tail t-test at alpha = 0.05/3).

identified as being hypersensitive to C16:0 PAF and/or L-PAF (in at least 2 out of three replicates), of which 25 deletion mutants encode multiple-drug resistance (MDR) genes whose deletions, are hypersensitive to a wide-variety of compounds (117, 120). The heterozygous diploid screen was performed in duplicate and 109 mutants were putatively identified as being hypersensitive to C16:0 PAF and/or L-PAF, 10 of which encode MDR genes (131). The isolation of the MDR deletion mutants suggested that the genome-wide screens were successful.

The C16:0 PAF and L-PAF sensitivity of the putative hits were confirmed by automated growth curve analysis at 40μM. This sub-lethal dosage had a mild effect on wildtype (Figure 6) and was selected for confirmation purposes as it provides for a stringent and sensitive way to detect and differentiate mild and strong sensitivities. In total, 23 haploid deletion mutants and 30 heterozygous diploid deletion mutants were confirmed to be sensitive to C16:0 PAF and/or L-PAF respectively (Tables 1 and 2). As expected from the growth curves results (Figure 6) that showed differences between PAF and L-PAF. I also saw more deletion mutants that were sensitive to PAF compared to L-PAF in my confirmed hits. I also expected that the heterozygous diploid screen would yield even fewer L-PAF hits. Indeed, there was a higher overlap between PAF and L-PAF hits in the haploid screen than in the diploid screen (Figures 9 and 10). It should be noted that *MTC4* is more sensitive to L-PAF and more *resistant* to PAF than wildtype while all other hits show sensitivity to one or both compounds.

Since chemical genetic interactions can be used as a method to predict mode-of-action of a compound (131), I analyzed the confirmed PAF/L-PAF sensitive mutant strains based on their gene ontology (GO) processes. This is done in order to group genes

Table 1. PAF and L-PAF confirmed chemical-genetic interactions.

ORF/NAME	PAF area fold decrease*	L-PAF area fold decrease*	Human Ortholog**	Cellular Function***
YKR031C/SPO14$^{\Psi}$	7.49	1.47	PLD1/2	Phospholipase D, sporulation, mating projections
YDL133W$^{\Psi}$	6.67		-	Needed for LACS activation and cell-cell fusion during mating
YGR240C/PFK1	4.53	1.21	PFKM	Subunit of phosphofructokinase
YBL094C	4.36		-	Dubious/not-expressed. overlaps YBL095w (unknown)
YHR039C-B/VMA10	4.33	4.33	-	Vacuolar H+ ATPase; Vacuolar acidification
YBR200W/BEM1	4.14	1.40	SH3PXD2A	Cell polarity; delocalized actin
YBR132C/AGP2	3.84	3.42	SLC7A8	Permease; carnitine transporter, spermidine uptake
YHL025W/SNF6	3.80	2.98	-	Subunit of SWI/SNF. Sporulation
YPL129W/TAF14	3.77	2.60	MLLT1/YEATS4	Complex with NuA3, TFIID, and RSC. Shmoos formation. Actin organization
YMR038C/CCS1$^{\Psi}$	3.77	1.88	CCS	Copper chaperone for superoxide dismutase Sod1p
YDR207C/UME6	3.29		TRIOBP	Transcriptional regulator; complex with Ime1p and Sin3p-Rpd3p
YGR167W/CLC1	2.61	2.58	LCa/LCb	Clathrin light chain, endocytosis, actin dynamics
YLL049w/LDB18	2.59		p24	Protein of unknown function. Meiosis. Spindle orientation; Component of Dynactin Complex.
YBL011W/SCT1$^{\Psi}$	2.06	1.69	-	Glycerol-3-phosphate acyltransferase. Prefers C16 over C18. makes Lyso-PA
YDL116W/NUP84	1.67	6.67	NUP107	Nuclear pore complex (NPC), Sporulation
YLR087C/CSF1	1.62	2.92	-	Fermentation at low temperature. Salt sensitive
YPR139C/VPS66	1.57	2.33	-	Vacuolar protein sorting. Defective Prc1p/Pep3p trafficking
YKL139W/CTK1		2.76	CRKRS	Catalytic subunit of CTDK-I that phosphorylates Rpo21p
YBR266C/SLM6		2.03	-	Actin organization; Synthetic lethal with PI4K
YBR255W/MTC4	0.63	1.36	-	Protein of unknown function. Life span abnormal. Telomere capping
YEL050C/RML2	1.20	1.80	MRPL2/RPL8	Mitochondrial ribosomal protein
YIL025C	1.27		-	Dubious
YLR065C	1.81	1.51	-	Unknown function. Sporulation

Ψ Indicates that the strain was confirmed by PCR and/or by re-making the knockout in house

* Blanks indicate no change; Fold decrease in area under the curve for each mutant compared to WildType on that day as calculated by the formula: [(Area Treated / Area Control)$_{WT}$ / (Area Treated / Area Control)$_{MUTANT}$]

** Human Orthologs based on pre-computed blast results from www.proteome.com show that 52% of my hits have orthologs as compared to ~31% in the yeast genome (132).

*** Adapted from the Saccharomyces Genome Database (www.yeastgenome.org)

Table 2. PAF and L-PAF confirmed drug-induced halpoinsufficiency interactions.

ORF/NAME	PAF area fold decrease*	L-PAF area fold decrease*	Human Ortholog**	Cellular Function***
YKR031C/SPO14	3.11		PLD1/2	Phospholipase D, sporulation, mating projections
YBL011W/SCT1	3.07	1.38	-	Acylation of glycerol-3-phosphate, prefers C16
YGL232W/TAN1	2.88	1.57	THUMPD1	tRNA acetyltransferase
YLR293C/GSP1	2.42		RAN	Nucleocytoplasmic transport (ran family), mitotic spindle formation
YLR373C/VID22	2.32		-	Transports FBPase from the cytosol to Vid vesicles
YMR032W/HOF1	1.95		STAC	Cytokinesis; regulates actomyosin ring dynamics and septin localization
YDR507C/GIN4	1.85	1.45	PRKAA2	Kinase involved in bud growth and assembly of the septin ring
YER118C/SHO1	1.82		DBNL	Transmembrane osmosensor, activation of the HOG pathway
YBL062W	1.78		-	Dubious. overlaps with SKT5
YOL127W/RPL25	1.76	1.46	RPL23A	Ribosomal protein (60S), Multiple buds, nuclear division defect. Nuclear export needs gsp1
YBR118W/TEF1	1.75	1.45	EEF1A1	Translational elongation factor EF-1alpha. Actin cable organization
YIL015C-A	1.73		-	Uncharacterized
YGR114C	1.72		-	Dubious
YAR018C/KIN3	1.62		NEK2	Kinase; no known role
YFR054C	1.56	1.48	-	Dubious
YDL133W	1.44		-	Needed for LACS activation and cell-cell fusion during mating
YHR143W-A/RPC10	1.43		POLR2K	RNA polymerase subunit
YKR067W/GPT2	1.41		-	Acylation of glycerol-3-phosphate, prefers C18
YPL143W/RPL33A	1.4	1.72	RPL35A	Ribosomal protein (60S)
YDR156W/RPA14	1.36		-	RNA polymerase I subunit A14
YJL186W/MNN5	1.35		-	Alpha-1,2-mannosyltransferase; localized to Golgi
YER157W/COG3	1.35	1.28	COG3	Component of the oligomeric Golgi complex (Cog1p through Cog8p)
YJL182C	1.3		-	Dubious
YOL145C/CTR9	1.27		CTR9	Component of the Paf1p complex
YCR006C	1.25		-	Dubious
YNL164C/IBD2	1.24		-	Spindle checkpoint pathway
YOR202W/HIS3	1.23	1.21	-	Histidine biosynthesis
YNL112W/DBP2	1.2	1.62	DDX17	ATP-dependent RNA helicase
YKL128C/PMU1	1.2		-	Putative phosphomutase
YFL008W/SMC1		1.38	SMC1A	Subunit of cohesin complex

* Blanks indicate no change; Fold decrease in area under the curve for each mutant compared to WildType on that day as calculated by the formula: [(Area Treated / Area Control)$_{WT}$ / (Area Treated / Area Control)$_{MUTANT}$]

** Human Orthologs based on pre-computed blast results from www.proteome.com show that 50% of my hits have orthologs as compared to ~31% in the yeast genome (132).

*** Adapted from the Saccharomyces Genome Database (www.yeastgenome.org)

with similar functions and assess the dataset for enrichments in any given process. For example, I had expected to find genes involved in lipid metabolism. I saw enrichments in genes implicated in cytoskeleton, sporulation, and transcription (Figures 9 and 10). Only three genes were identified in both the haploid and the diploid screens: *SPO14*, *SCT1*, *YDL133w*. The first two are involved in phospholipid metabolism and the third is an uncharacterized gene.

3.5 C16:0 PAF Causes Actin Cytoskeleton Defects And Leads To Spindle Misorientation And Binucleate Cells

Mammalian studies of PAF show a link between PAF and F-actin polymerization/depolymerization oscillations (64-66). My yeast chemical genomic screens identified numerous cytoskeleton related genes, which suggests that similar to man, PAF treatment of yeast may impact actin cytoskeleton. To explore this hypothesis using rhodamine-phalloidin staining (127) I visualized the effect of C16:0 PAF treatment on the actin cytoskeleton.

Normally, the F-Actin cytoskeleton is polarized towards the site of an emerging bud with actin patches at much higher levels in the bud. The cables extend from the bud into the mother cell (128) (Figure 11 ethanol control). In my pilot study, I found that some PAF treated cells in S-phase (mini-budded) show an abnormal actin phenotype as compared to both ethanol and L-PAF cultures. This preliminary data (n=1) shows a large increase in S-phase cells having abnormal actin compared to carrier treated cells (Figure 11). This affect drops when observing cells in all stages of cell cycle including those stages that have no observable actin cables normally. I defined "abnormal actin" as a lack in polarity, diffuse staining in the cytoplasm, and a lack in cables.

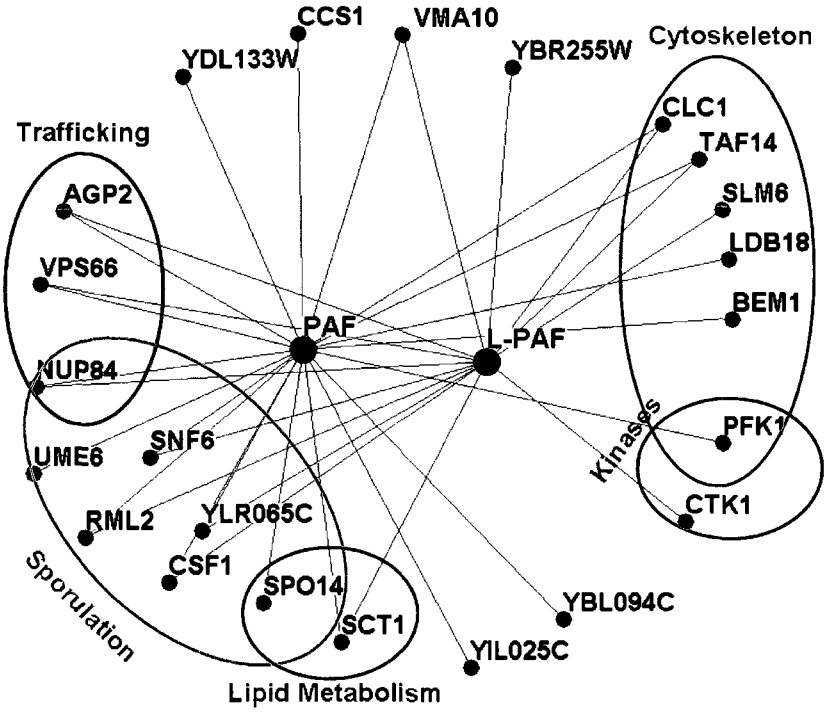
CCS1
VMA10
YDL133W
YBR255W
Cytoskeleton
CLC1
Trafficking
TAF14
AGP2
SLM6
LDB18
VPS66
BEM1
PAF
L-PAF
NUP84
PFK1
Kinases
SNF6
UME6
CTK1
RML2
YLR065C
CSF1
SPO14
YBL094C
Sporulation
SCT1
YIL025C
Lipid Metabolism

Figure 9. C16:0 PAF and L-PAF chemical-genetic hits show enrichments for cytoskeleton and sporulation related functions. Chemical-genetic interactions for PAF and L-PAF are indicated by blue lines. Circles highlight genes involved in certain biological process (based on GO process).

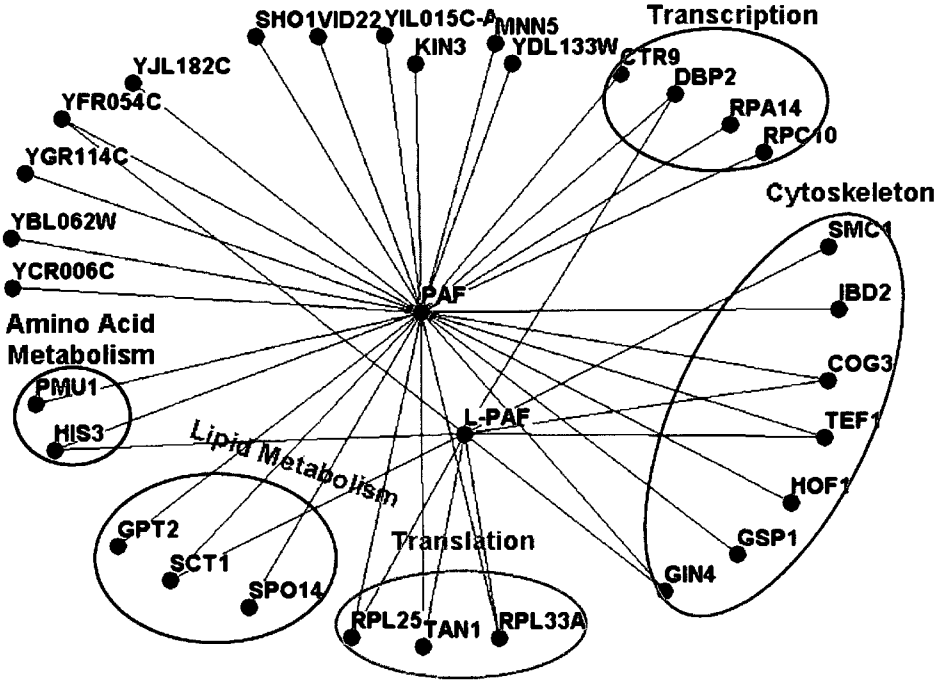
SHO1
VID22
YIL015C-A
MNN5
KIN3
YDL133W
Transcription
CTR9
DBP2
RPA14
RPC10
YJL182C
YFR054C
YGR114C
YBL062W
YCR006C
Cytoskeleton
SMC1
IBD2
PAF
Amino Acid
Metabolism
COG3
PMU1
HIS3
L-PAF
TEF1
Lipid Metabolism
HOF1
GPT2
SCT1
SPO14
Translation
GSP1
GIN4
RPL25
TAN1
RPL33A

Figure 10. C16:0 PAF and L-PAF drug-induced haploinsufficiency hits show enrichments for cytoskeleton related functions. Interactions for PAF and L-PAF are indicated by blue lines. Circles highlight genes involved in certain biological process (based on GO process).

It is known that F-Actin disruption is a cause of spindle misorientation because astral microtubules are linked to actin cables and aid in orienting the spindle (53, 55). This disruption causes an increase in binucleate mother cells due to the separation of the sister genomes within that same mother cell (53). Further, one of the hits in the screens was a spindle checkpoint mutant, *IBD2*, which plays it role upstream of the two major spindle position checkpoint controlling proteins, *BUB2* and *BFA1,* and displays spindle orientation defects upon deletion (58). Hence, I was interested in determining if PAF treatment results in a spindle orientation defect or an increase in binucleate mother cells. To test this, through genetic manipulation I created a wildtype strain expressing a GFP tagged *TUB1,* the α-tubulin component, which allowed me to visualize microtubules by fluorescent microscopy. This strain was subjected to fluorescent microscopy after treatment with PAF or L-PAF and staining the DNA with DAPI. The samples were compared to carrier treated cultures. I found that 66% of the cells in S-phase of cell cycle (having a small bud and spindle) exhibited misoriented spindle upon PAF treatment as compared to 25% and 23% for wildtype and L-PAF, respectively. This is a 2.5-fold increase in misoriented spindle in PAF treated cultures as compared to wildtype (Figure 12). Remarkably, 30% of the large budded cells that completed anaphase exhibited a binucleate mother cell phenotype as compared to 0% in carrier treated cells and 2% in L-PAF treated cells (Figure 13). This suggests that PAF greatly affects the yeast cytoskeleton causing spindle misorientation and leading to DNA loss. This would explain PAF's cytotoxic effect.

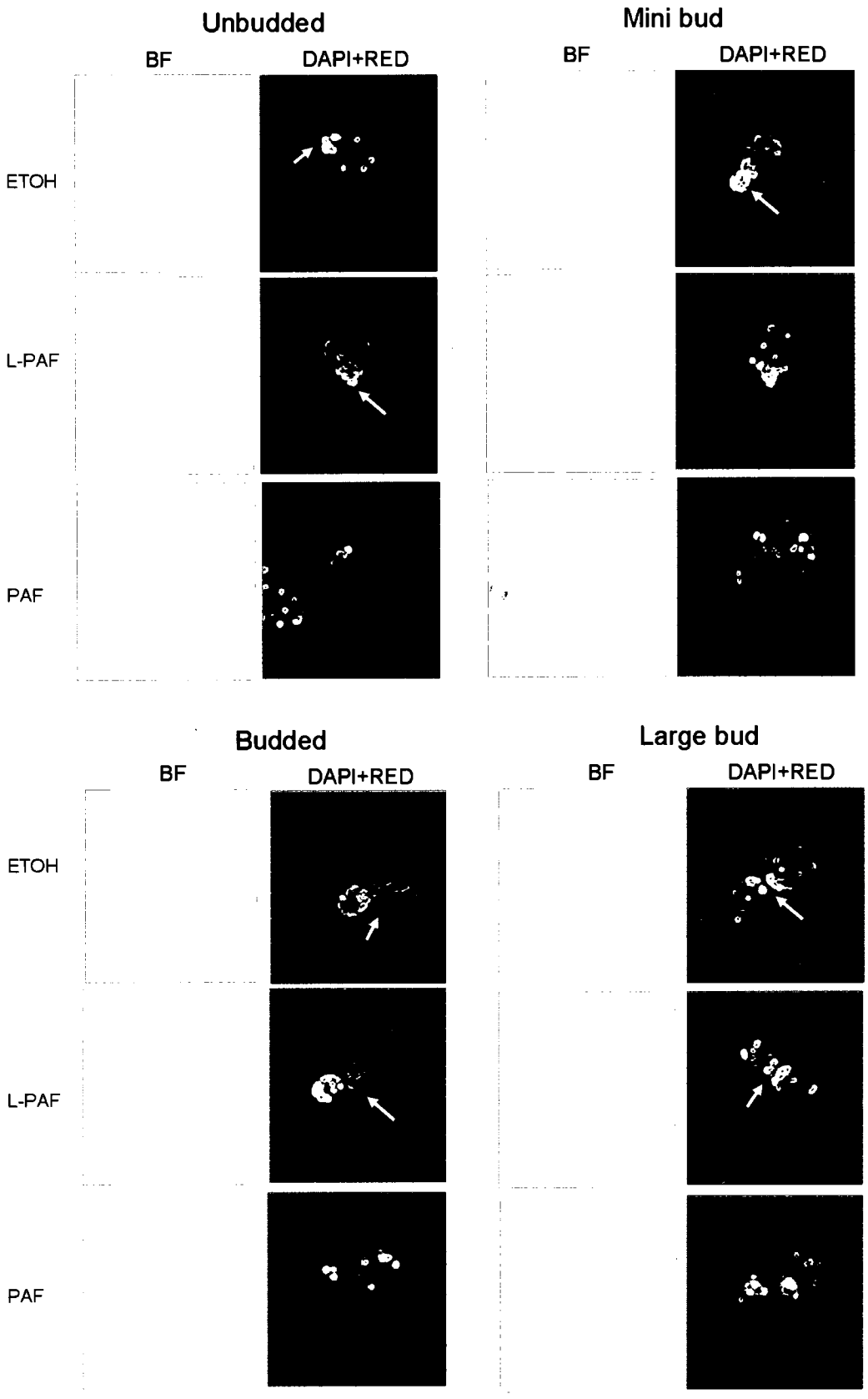
Unbudded
BF
DAPI+RED
ETOH
L-PAF
PAF
Mini bud
BF
DAPI+RED
Budded
BF
DAPI+RED
ETOH
L-PAF
PAF
Large bud
BF
DAPI+RED

Figure 11. C16:0 PAF causes actin cytoskeleton defects. *MAT*a wildtype (YKB779) cells were incubated at 25°C in the presence or absence of 180μM C16:0 PAF or L-PAF for 4 hours. The cells were fixed and stained with both DAPI and rhodamine-conjugated phalloidin and imaged with a Leica fluorescent microscope as described in the materials and methods. Fluorescent optical sections with a total thickness of 5μm were collapsed into two dimensions (127). PAF treated S-phase cells show an increase in cells having abnormal actin compared to carrier treated cells. Cells with "normal" actin were defined as those cells having cables between the mother cell and bud, asymmetrically distributed actin patches, and actin at the septin ring. Cells with "abnormal" actin were defined as those cells having similar numbers of actin patches in the mother cell and bud (lacking polarity), diffuse staining in the cytoplasm, and no cables. White arrows indicate actin patches in the bud, actin cables, and actin at the septin ring. Images were enhanced using "detect edges" option in IrfanView software.

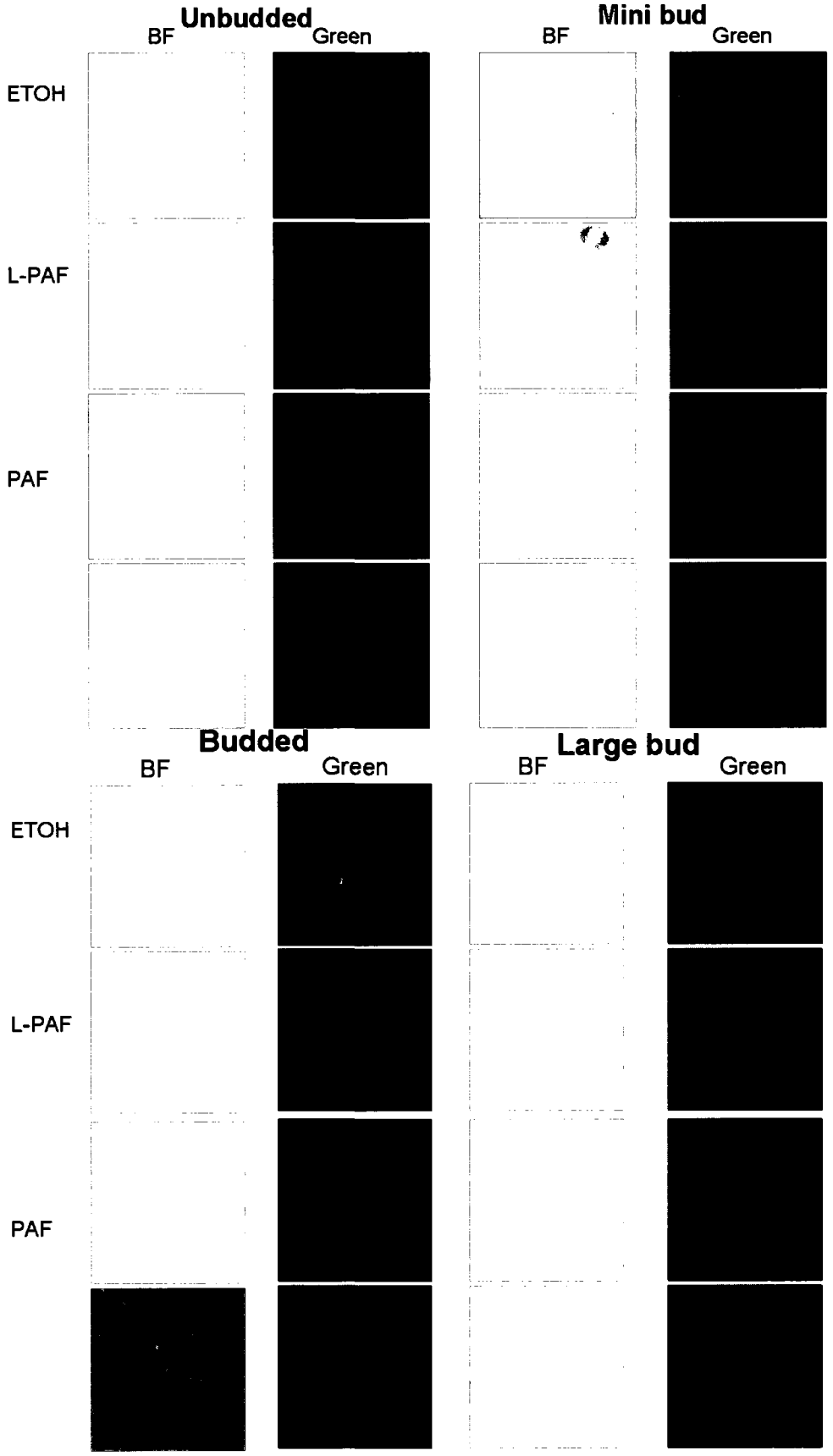
Unbudded
BF
Green
Mini bud
BF
Green
ETOH
L-PAF
PAF
Budded
BF
Green
Large bud
BF
Green
ETOH
L-PAF
PAF

Figure 12. C16:0 PAF causes spindle mis-orientation. Yeast cells with GFP-TUB1 integrated in the genome (YKB1191) were incubated in Triplicate at 25°C in the presence or absence of 180μM C16:0 PAF or L-PAF for 4 hours. The cells were fixed then imaged with a Leica fluorescent microscope. Small budded cells (or S-phase) exhibit a 2.5-fold increase in mis-oriented spindle upon PAF treatment as compared to carrier treated cells. Misoriented spindles were defined as those in which the spindle axis does not pass through the neck.

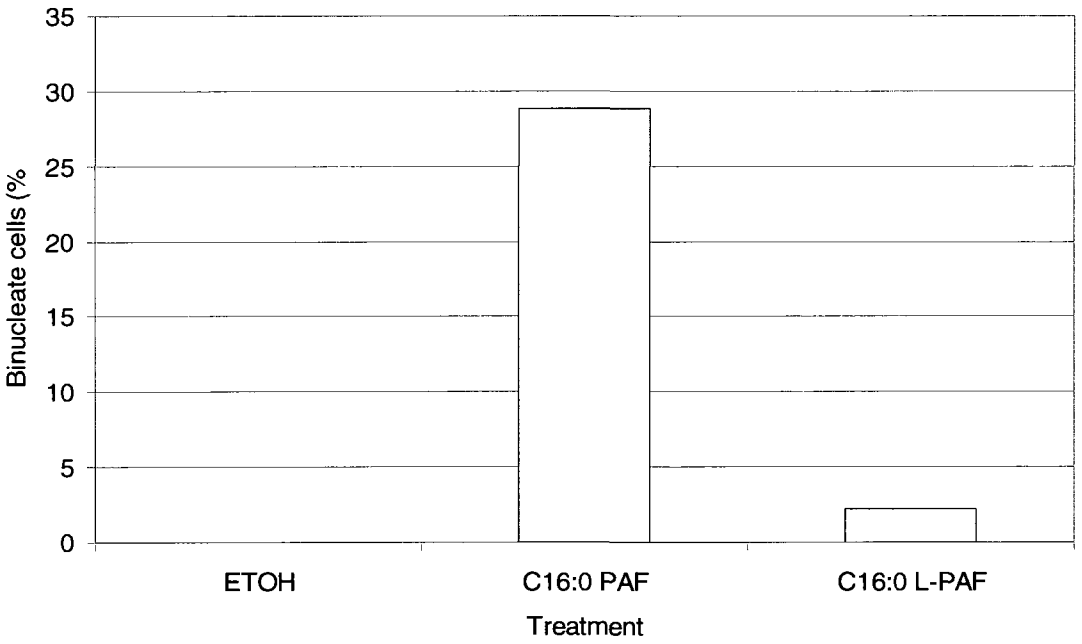
35
30
25
20
15
10
5
0
Binucleate cells (%
ETOH
C16:0 PAF
C16:0 L-PAF
Treatment

Figure 13. C16:0 PAF causes chromosomal DNA to segregate in the mother cell. *MAT*a wildtype (YKB779) cells were incubated at 25°C in the presence or absence of 180μM C16:0 PAF or L-PAF for 4 hours. The cells were fixed and stained with DAPI and imaged with a Leica fluorescent microscope as described in the materials and methods. I found that 30% of the large budded cells exhibit a binucleate cell body phenotype as compared to 0% in carrier treated cells and 2% in L-PAF treated cells. This was calculated by dividing the number of cell in which the two sister genomes separated but both remained in the mother cell by the total number of cells that had completed anaphase (large budded).

3.6 *ydl133wΔ* Mutants Are Sensitive To 40μM C16:0 PAF

I was interested in identifying genes that were only sensitive to PAF as I expected those to have direct bearing on the human PAF effects. *YDL133w*, one of the mutants that was identified in both the haploid and the diploid screens, exhibited a very strong sensitivity to PAF and not L-PAF. This uncharacterized gene has been shown in high-throughput studies to be required for calcium influx during mating such that it is needed to activate the low affinity calcium influx system (LACS) (133). As PAF treatment elicits increases in free intracellular calcium in mammalian cells (134), I was particularly interested in characterizing the function of Ydl133wp in PAF response. Since mis-annotated genes exist with in the commercial deletion mutant arrays (30), I set out to confirm the hypersensitivity of *ydl133wΔ* cells to C16:0 PAF. Using standard PCR methods (125) I constructed a *ydl133wΔ* mutant strain. Using growth curve analysis I confirmed that *ydl133wΔ* cells are hypersensitive to PAF but not L-PAF (Figure 14).

3.7 *ydl133wΔ* SL-SGA Screen

To gain insight into the function of the uncharacterized Ydl133wp, I performed a genome-wide synthetic lethal SGA (see introduction). This serves to uncover functional relationships and thus predict the function of *YDL133w*. The *ydl133wΔ* SL-SGA screen was performed in triplicate and after removing 12 linkage group deletion mutants and non-specific slow-grower mutants, a list of 108 putative deletion mutants with synthetic interactions with *ydl133wΔ* was generated. As high-throughput SL-SGA screening produces a high rate of false positives (40) I confirmed these interactions by tetrad

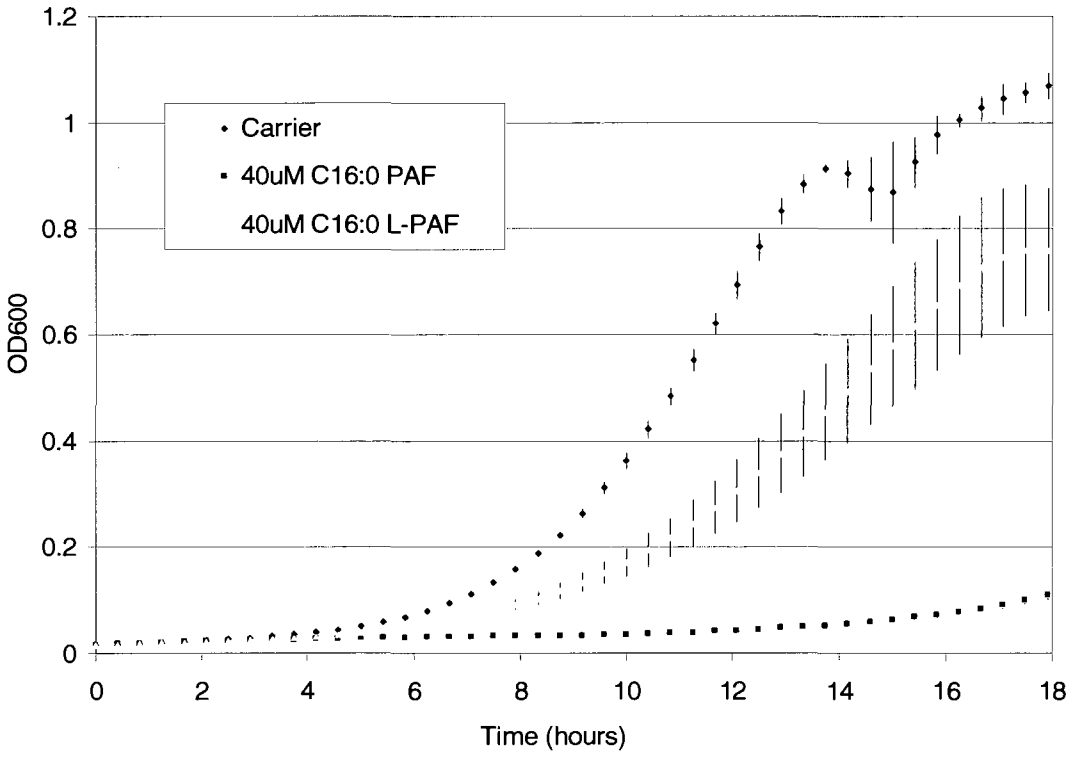
1.2
1
0.8
0.6
0.4
0.2
0
OD600
Carrier
40uM C16:0 PAF
40uM C16:0 L-PAF
0
2
4
6
8
10
12
14
16
18
Time (hours)

Figure 14. *ydl133wΔ* mutants are sensitive to 40μM C16:0 PAF. Automated yeast growth curve of *MATα ydl133wΔKanMX* (YKB1164) showing OD_{600} as a function of time in hours. Cultures were grown in YPD in triplicate and treated with ethanol carrier, 40μM C16:0 PAF, or 40μM C16:0 L-PAF dissolved in ethanol. OD_{600} measurements of the samples were taken every 25 minutes in a plate-reader (Multiskan Ascent, Thermo Labsystems).

dissection and 15 deletion mutants were identified that displayed synthetic genetic interactions with *ydl133wΔ* (Table 3).

3.8 Attempted Localization of Ydl133wp

The amino acid sequence of Ydl133wp indicates that is has four transmembrane domains near its C-terminus. The Yeast Resource Center (http://www.yeastrc.org/pdr/viewProtein.do?id=529222) lists 7 unpublished yeast-2-hybrid interactions with Ydl133w, three of which play a role in the endoplasmic reticulum or have been localized to there by GFP tagging (98). This hints that Ydl133wp could be in the endoplasmic reticulum membrane. Therefore, I sought to determine its subcellular localization of Ydl133w by two complimentary methods, GFP fusions and indirect immunofluorescence.

First, using standard PCR based methods (125) I made a C-terminal GFP fusion protein at the endogenous *YDL133w* gene locus. The successful fusion was confirmed by PCR (data not shown). Although the fusion was confirmed I could not detect a signal on the fluorescent microscope (data not shown) and this experiment was deemed unsuccessful.

In a second attempt to localize Ydl133w, I sought to perform indirect immunofluorescence. To do this, through standard PCR based methods I C-terminally tagged Ydl133w with a Myc tag and confirmed the expression of the fusion by western blotting (Figure 15). This strain, along with wildtype untagged controls was subjected to immunofluorescence. Only background signal was observed on the fluorescent microscope as can be seen in Figure 16.

Table 3. *ydl133wΔ* confirmed SSL genetic interactions.

ORF/Name	Interaction type*	Ortholog**	Cellular Function***
YOR303W/CPA1	mild SS	CAD	arginine biosynthesis pathway
YJL071W/ARG2	mild SS	-	arginine biosynthesis pathway
YOL058W/ARG1	mild SS	ASS1	arginine biosynthesis pathway
YER069W/ARG5,6	SS	-	arginine biosynthesis pathway
YJL088W/ARG3	mild SS	OTC	arginine biosynthesis pathway
YOR312C/RPL20B	SS	RPL18A	component of the large (60S) ribosomal subunit
YGR162W/TIF4631	SS	eIF-4GII-isoform1	Translation initiation factor eIF4G. Interacts with Tif1p and Pab1p.
YNL284C/MRPL10	SS	MRPL10	Mitochondrial ribosomal protein of the large subunit
YNL170W	mild SS	-	Dubious ORF. overlaps PSD1
YDR126W/SWF1	SS	ZDHHC17	Palmitoyltransferase that acts on many SNAREs. role in vacuole fusion and polarized actin cables
YHL031C/GOS1	SL	GOS-28/GOSR1	v-SNARE protein involved in Golgi transport
YER083C/GET2	SS	-	Part of GET complex. Retrieval of HDEL proteins from the Golgi to the ER
YLR261C/VPS63	SS	-	Dubious ORF. Overlaps YPT6
YLR039C/RIC1	SS	-	Transport to the cis-Golgi network. heterodimer with Rgp1p acts as a GTP exchange factor for Ypt6p
YDR477W/SNF1	mild SS	PRKAA2/ MELK/NUAK2	AMP-activated protein kinase. binds Ctk1p

*SS=synthetic sick, SL=synthetic lethal.

**Human Orthologs based on pre-computed blast results from www.proteome.com show that 60% of my hits have orthologs as compared to ~31% in the yeast genome (132).

***Adapted from the Saccharomyces Genome Database (www.yeastgenome.org)

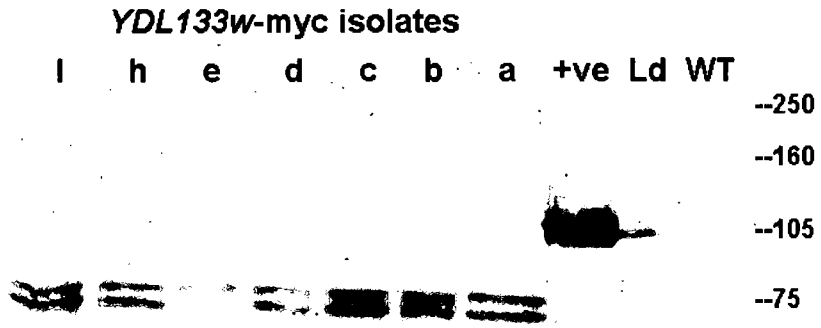
YDL133w-myc isolates
l h e d c b a +ve Ld WT
--250
--160
--105
--75

Figure 15. c-Myc tagging of *YDL133w* was confirmed by western blotting. Whole cell extracts (WCE) were prepared and the proteins separated by SDS-PAGE then probed by anti-Myc as the primary antibody as indicated. Western blot of 7 isolates of *YDL133w*-Myc shows expression of the fusion protein at the expected size (74kDa). The positive control (+ve) was a Myc tagged *EAF7* with an expected running size = 100kDa. Ld= Ladder; WT=wildtype; letters indicate isolates tested.

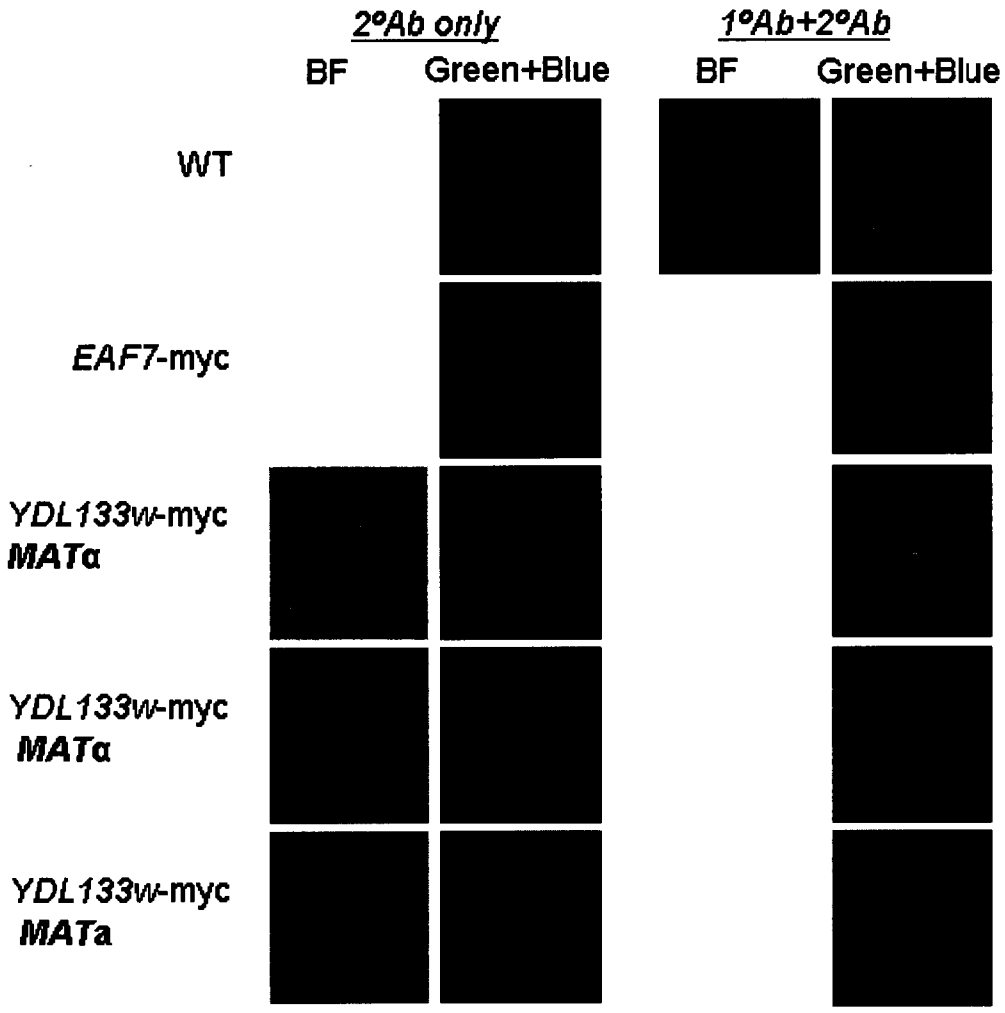
2°Ab only
1°Ab+2°Ab
BF
Green+Blue
BF
Green+Blue
WT
EAF7-myc
YDL133w-myc
MATα
YDL133w-myc
MATα
YDL133w-myc
MATa

Figure 16. Indirect immunofluorescence does not point to the localization of *YDL133w*. Determination of subcellular localization of *YDL133w* by Indirect Immunofluorescence. c-myc tagged *YDL133w* yeast strains were stained by either secondary antibody or by both primary and secondary antibody and imaged on a Leica fluorescent microscope. (See Materials and Methods for details). *EAF7*-myc is included as a positive control and shows an overlap of Green and DAPI signals indicating nuclear localization as expected.

3.9 Preliminary Lipidomics Profiling

One interpretation of the yeast hypersensitivity to PAF is that either yeast are not sensitive to PAF, but the media may contain enzymes that act on PAF and it is the by-product which is mediating the toxic events. Indeed, the manufacturers of the YPD ingredients provided information about the animal sources used in making their BactoPeptone that leads us to suspect that the BactoPeptone ingredients could contain PAF-AH. To address this possibility I collaborated with the Bennett and Figeys labs at the University of Ottawa to perform lipidomics profiling which uses tandem mass spectrometry to select the ion of interest, fragment the molecule, and then separate the fragment ions on the basis of their m/z value. This allows for identification of the molecule and insight into its structure (121). I treated media alone or cells in the media with ethanol, PAF, or L-PAF and then extracted the phospholipids from the media, cell pellet, and supernatant of each treatment as described in the materials and methods. The phosphocholine containing lipids were analyzed by mass spectrometry. A C13 LPC was spiked before lipid extraction to serve as an internal standard in all the samples. This data is considered preliminary because the experiment was done in singlet. My results suggest that the media does not contain enzymes that affect the integrity of PAF or L-PAF (Figure 17a).

Alternatively, it is possible that PAF maybe mediating its effect solely externally, therefore I was interested in confirming that PAF and L-PAF were internalized. Further, as I saw some overlap in the PAF and L-PAF chemical genomic screens (Figures 9 and 10) as well as weak sensitivity of wildtype cells to L-PAF, I was interested in determining if this could be attributed to the conversion of L-PAF to PAF by an enzyme

in yeast (83, 96). I found that the compounds do enter the cells and a large proportion of L-PAF is acetylated to PAF (Figure 17b), which is released by the cells presumably by secretion or upon death (Figure 17c).

Further, I was interested in knowing if PAF treatment was eliciting changes in overall phosphocholine-containing-glycerophospholipid levels thus causing an effect that may not be specific to PAF signalling. When profiling all detectable phosphocholine lipids, I found 19 species that had quantifiable peaks in both PAF and ethanol treated cells and allows for a broader look at changes in lipids upon treatment. It was found that apart from the aforementioned changes there were no major changes in these 19 lipids upon treatment with either PAF or L-PAF (Figure 18).

These results, although preliminary, suggest that yeast are able to convert C16:0 L-PAF to C16:0 PAF and that the effects of C16:0 PAF are specific to this molecule. This work also indicates that lipidomics may be an excellent tool for the dissection of PAF cellular effects.

A

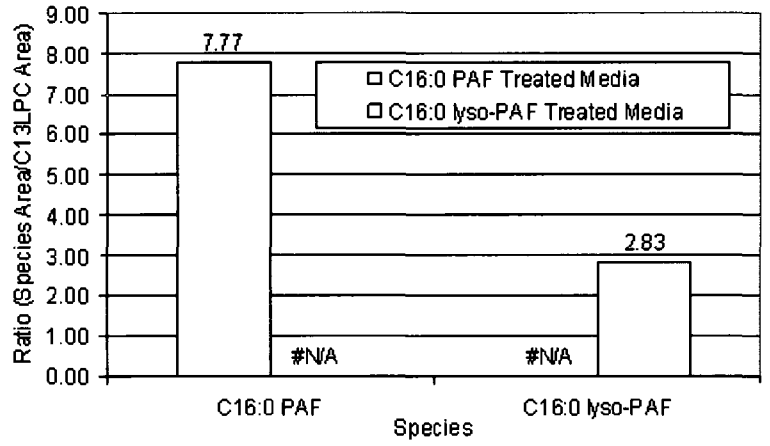
9.00
8.00
7.00
6.00
5.00
4.00
3.00
2.00
1.00
0.00
Ratio (Species Area/C13LPC Area)
7.77
2.83
#N/A
#N/A
C16:0 PAF Treated Media
C16:0 lyso-PAF Treated Media
C16:0 PAF
C16:0 lyso-PAF
Species

B

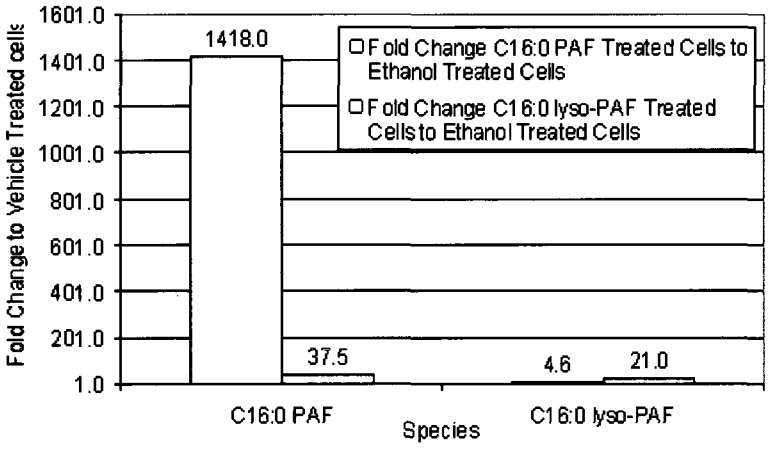
1601.0
1401.0
1201.0
1001.0
801.0
601.0
401.0
201.0
1.0
Fold Change to Vehicle Treated cells
1418.0
37.5
4.6
21.0
Fold Change C16:0 PAF Treated Cells to Ethanol Treated Cells
Fold Change C16:0 lyso-PAF Treated Cells to Ethanol Treated Cells
C16:0 PAF
C16:0 lyso-PAF
Species

C

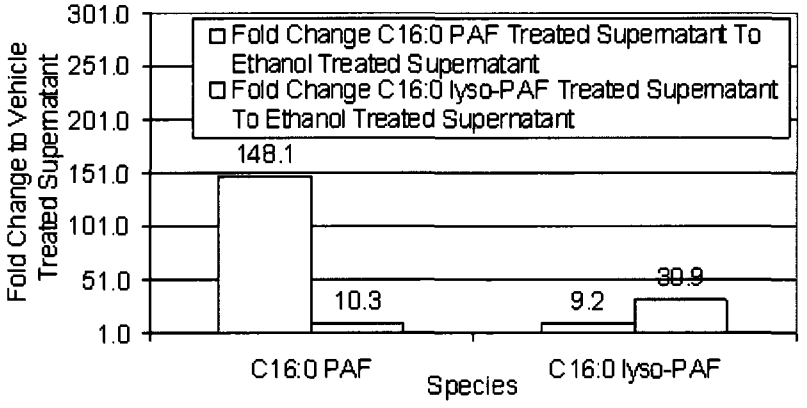
301.0
251.0
201.0
151.0
101.0
51.0
1.0
Fold Change to Vehicle Treated Supernatant
148.1
10.3
9.2
30.9
Fold Change C16:0 PAF Treated Supernatant To Ethanol Treated Supernatant
Fold Change C16:0 lyso-PAF Treated Supernatant To Ethanol Treated Supernatant
C16:0 PAF
C16:0 lyso-PAF
Species

Figure 17. Mass Spectrometry hints that C16:0 PAF and L-PAF are stable in YPD alone but are possibly hydrolyzed and acetylated inside the cells, respectively. Samples were treated with compounds for 13.75 hours at 25°C then the lipids were extracted and total lipids were analyzed using a 2000 Q TRAP mass spectrometer. A precursor ion scan for phosphocholine (m/z 184) was used to focus in on phosphocholine containing lipids (see Materials and Methods). A) Rich media (YPD) was analyzed by mass spec after treatment with carrier, 40uM C16:0 PAF or L-PAF and shows that one species remains undetectable when treating with the other. B) Fold change for cells treated with either PAF or L-PAF as compared to carrier treated cells indicates that PAF is either in or on the cells and that L-PAF maybe acetylated to PAF. C) Fold change for supernatant of samples treated with either PAF or L-PAF as compared to carrier treated cells indicates that some PAF/L-PAF is detected in the supernatant with some breakdown of PAF and acetylation of L-PAF. (N=1).

A

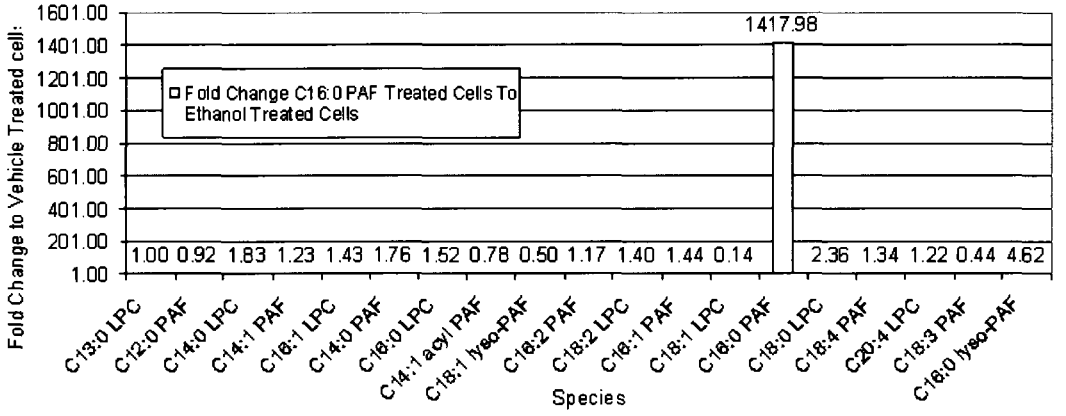
Fold Change to Vehicle Treated cell:
1601.00
1401.00
1201.00
1001.00
801.00
601.00
401.00
201.00
1.00
Fold Change C16:0 PAF Treated Cells To Ethanol Treated Cells
1417.98
1.00 0.92 1.83 1.23 1.43 1.76 1.52 0.78 0.50 1.17 1.40 1.44 0.14
2.36 1.34 1.22 0.44 4.62
C13:0 LPC
C12:0 PAF
C14:0 LPC
C14:1 PAF
C16:1 LPC
C14:0 PAF
C16:0 LPC
C14:1 acyl PAF
C18:1 lyso-PAF
C18:2 PAF
C18:2 LPC
C16:1 PAF
C18:1 LPC
C16:0 PAF
C18:0 LPC
C18:4 PAF
C20:4 LPC
C18:3 PAF
C16:0 lyso-PAF
Species

B

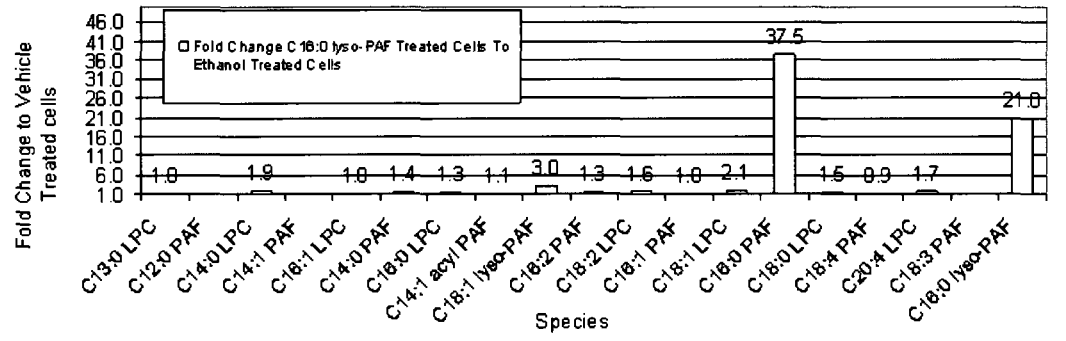
Fold Change to Vehicle Treated cells
46.0
41.0
36.0
31.0
26.0
21.0
16.0
11.0
6.0
1.0
Fold Change C16:0 lyso-PAF Treated Cells To Ethanol Treated Cells
37.5
21.0
1.0 1.9 1.0 1.4 1.3 1.1 3.0 1.3 1.6 1.0 2.1
1.5 0.9 1.7
C13:0 LPC
C12:0 PAF
C14:0 LPC
C14:1 PAF
C16:1 LPC
C14:0 PAF
C16:0 LPC
C14:1 acyl PAF
C18:1 lyso-PAF
C18:2 PAF
C18:2 LPC
C16:1 PAF
C18:1 LPC
C16:0 PAF
C18:0 LPC
C18:4 PAF
C20:4 LPC
C18:3 PAF
C16:0 lyso-PAF
Species

Figure 18. Mass Spectrometry lipid profiling data indicates that treating with C16:0 PAF and L-PAF does no elicit detectable changes in phosphocholine containing lipids in yeast. Samples were treated with compounds then the lipids were extracted and total lipids were analyzed using a 2000 Q TRAP mass spectrometer. A precursor ion scan for phosphocholine (m/z 184) was used to focus in on phosphocholine containing lipids (see Materials and Methods). A) Fold change for cells treated with C16:0 PAF as compared to carrier treated cells shows that no major change in the composition of other phosphocholine containing lipids occurs upon treatment. B) Fold change for cells treated with C16:0 L-PAF as compared to carrier treated cells shows that no major change in the composition of other phosphocholine containing lipids occurs upon treatment. (N=1).

CHAPTER 4: DISCUSSION

In this study, I have shown that similar to mammalian cells, treatment of *Saccharomyces cerevisiae* with exogenous C16:0 PAF results in cytotoxicity and decreased viability. I exploited this phenotype to perform a series of PAF chemical-genomic screens in order to uncover cellular pathways affected by PAF and to shed light on the PAFR-independent mode-of-action. The screens implicated a role for C16:0 PAF in cytoskeletal stability and spindle orientation. Importantly, the screens identified many cellular processes that were previously linked to PAF function in mammalian cells and identified new potential roles for PAF.

4.1 Yeast As A Model For PAF Cytotoxicity

In the brain, PAF at high levels can be neurotoxic and can mediate cell loss in many diseases (5, 7-11, 61, 73-78). C16:0 PAF neurotoxicity can occur through an unknown PAF-receptor (PAFR)-independent pathway while its metabolite, C16:0 L-PAF, is not neurotoxic (60, 80). PAF has been detected in yeast (91, 92) along with some of the enzymes in the synthesis pathway which argues that yeast may be a good model for PAF studies even though the biological role in yeast is not known. To my knowledge, and probably due to L-PAF's inactivity, no one has detected L-PAF in yeast.

Using automated growth curves, I found that wildtype yeast are sensitive to C16:0 PAF in a dose-dependant manner (Figure 6), however, although yeast are sensitive to L-PAF, the sensitivity is significantly less. The minor sensitivity of wildtype yeast to L-

PAF may be explained by the fact that yeast have the enzyme to acetylate L-PAF to make PAF (83). Further, my lipidomics study supports the occurrence of the conversion of exogenous L-PAF to C16:0 PAF in yeast (Figure 17b).

While 6 hours of C16:0 PAF treatment caused decreases in viability, L-PAF treatment did not cause toxicity (Figure 8). Similarly, an analogous ether lipid, edelfosine, caused decreased viability in yeast and induced apoptosis in tumor cells (106, 108). This suggests that ether lipids that are bioactive or death-inducing in mammalian cells tend to have the same property in yeast confirming this organism as a potentially informative model for the investigation of lipid-signalling.

Previous studies indicate that PAF levels in yeast may be cell cycle regulated with higher levels of C16:0 PAF in G1 or M compared to S-phase (93), suggesting a possible role for PAF in some aspect of cell cycle progression. In agreement with this hypothesis, I found that exogenous C16:0 PAF treatment of wildtype cells results in a G1 delay (Figure 7). In contrast L-PAF treatment had no detectable effect on the cell cycle. These results are in line with mammalian studies of PAF that have shown similar effects upon cell cycle progression. For example, NRK cells (immortalized rat kidney fibroblasts) treated with PAF inhibited the G1 to S transition in these cells (67). Hence the parallels in PAF species toxicity, evidenced by biochemical pathway conservation and PAF cell cycle effects, suggest that *S. cerevisiae* may be a relevant model organism for the dissection of PAF signalling. As well, mice overexpressing the PAF receptor develop skin tumors (62) further implicating PAF in cell proliferation. In human T-cells, micromolar levels of PAF suppressed proliferation while L-PAF had no effect at these

concentrations. (68). My results parallel those of mammalian systems for both PAF and L-PAF and strongly suggest a role for PAF in cell cycle transitions.

The above results are quite interesting when combined together. The delay in cell cycle and the decrease in viability may be linked because I am treating with PAF for long periods of time. Indeed it has been shown in yeast that a prolonged exposure to cell cycle arresting chemicals can lead to cell death. For example, alpha-factor treatment of wildtype yeast for long periods of time can lead to cell death in up to 26% of the population (135, 136). This argues that the toxicity seen with PAF treatment is specifically through cell cycle delay.

Hence the parallels in PAF species toxicity, evidenced by biochemical pathway conservation and PAF cell cycle effects, suggest that *S. cerevisiae* may be a relevant model organism for the dissection of PAF signalling.

4.2 Yeast Chemical Genomic Screens

Chemical genomic screens are powerful tools for the analysis of drug mode-of-action. Despite the parallels in PAF-induced toxicity and phenotypes between man and yeast, no genome-wide screen on PAF or L-PAF had been conducted. In this study, I performed two yeast chemical genomic screens and identified 53 deletion mutants that are hypersensitive to either C16:0 PAF or L-PAF.

Several internal controls indicate that the screens were successful and produced specific chemical profiles. First, I had expected my putative hit lists to include "common hits" known as Multi-Drug Resistance genes (MDR). MDR genes are defined as genes that when deleted exhibit sensitivity to more than 20% of compounds (120, 131). In other words, these are genes needed for growth in the presence of multiple drugs. They are

thought to play roles in the development of anti-microbial resistance and are usually involved in processes such as intracellular trafficking, endosomal transport, vacuolar degradation, and transcription (131). The study of such genes has great medicinal value but for the purpose of my work, they were considered non PAF-specific effects and were subtracted out of the putative hit list. I found 25 and 10 of these for the chemical-genetic and haploinsufficiency screens respectively which suggest that technically the screen was working. Second, three deletion mutants (*SPO14*, *SCT1*, and *GPT2*) which had previously been demonstrated to be PAF and L-PAF sensitive (99), were identified in my screens (Tables 1 and 2). It is interesting to note that there were differences in sensitivity to the compounds in liquid versus solid media. For example, two genes (*SPO14* and *YBL094W)* exhibited sensitivity to both compounds on solid media (YPD with agar) but when tested in liquid media were only sensitive to PAF. This phenomenon was observed for edelfosine as well (105) and may be an indication that such lipids interact with the agar.

Third as wildtype yeast display increased sensitivity to C16:0 PAF compared to L-PAF (Figure 6). I anticipated that the C16:0 PAF chemical genetic network would be more extensive compared to L-PAF. Indeed, I saw nine out of 23 confirmed haploid deletion mutants displaying either sensitivity to PAF alone or increased sensitivity to PAF over L-PAF, 11 haploid deletion mutants sensitive to both compounds and only three haploid deletion mutants sensitive to L-PAF alone. The haploinsufficiency screen displayed similar trends. Of the 30 hits in this screen, 19 heterozygous deletion mutants were sensitive to PAF alone, with only one heterozygous deletion mutant sensitive to L-PAF alone. The remaining 10 mutants were sensitive to PAF with mild sensitivity to L-

PAF. The overlap between PAF and L-PAF sensitive strains may be explained by the fact that the L-PAF-AT enzyme is present in yeast and can convert L-PAF to PAF (83) and my preliminary lipidomics analysis supports this view (Figure 17). Although yeast can convert L-PAF to C16:0 PAF this reaction must be limiting, or the sensitivity of yeast to PAF and L-PAF would be similar. The identification of mutants that are equally sensitive to PAF and L-PAF suggest that these growth defects may not be specific to PAF-dependent signaling but secondary defects such as cell wall or vacuole function. For example *rml2Δ* cells were equally sensitivity to PAF and L-PAF. Rml2p is a mitochondrial ribosomal protein and probably a non-specific hit. In parallel, the identification of mutants sensitive to L-PAF alone suggests that L-PAF may have cellular implications that are not dependent on conversion to PAF. As my goal is to understand the specific C16:0 PAF neurotoxic effects, I was particularly interested in the mutants that displayed dramatic hypersensitivity to PAF compared to L-PAF.

Importantly, many of the deletion mutants identified in the screen encode proteins implicated in pathways/functions linked to PAF cellular effects. For example, I determined that PAF-treatment causes a G1 delay in yeast (Figure 7) and many mutants with cell cycle defects were identified in my screen. These include, *bem1Δ* (a scaffold protein implicated in budding that localizes to nascent bud sites to arrange actin cytoskeleton polarity) and *snf6Δ* (a subunit of SWI/SNF chromatin remodelling complex) mutants which both display G1 pile up (129). PAF treatment has also been shown to stimulate vacuolar ATPase and pyrophosphatase activities in isolated yeast vacuoles (100). The protein(s) involved in this PAF effect on vacuoles are not known. Coincidentally, a vacuolar proton ATPase, *VMA10*, was identified in my screens. Two

other vacuole related mutants were also identified in my haploid screens, *SWF1*, which has a role in vacuole fusion (137) and *VPS66* which is involved in vacuolar protein sorting based on a high throughput study (138). The ability of the PAF chemical genomic screens to identify genes implicated in known PAF-mediated cellular effects, G1 arrest and vacuole function, suggests that the screens are successful in predicting downstream PAF effects.

Many of the hits that were sensitive to PAF and not L-PAF were involved in pathways and processes similar to those implicated for PAF in mammalian systems. In rabbit lung injury caused by PAF treatment the addition of superoxide dismutase (SOD) augmented the PAF response (139). This suggested that the levels of superoxide radicals determine the response to PAF such that depletion of superoxide leads to excessive responses. Further, endothelial cells' permeability is affected by PAF such that intercellular gaps are formed and certain enzymes leaked out. This effect was partially decreased by pre-treatment with SOD (140). As well, human SOD was shown to reduce leukocyte adherence initiated by PAF in cat intestines (141). The effect of SOD in attenuating PAF-induced alterations of microcirculation in dog stomachs was assessed and showed that SOD significantly reduced the responses (142). In agreement with the role of SOD in the PAF response I identified *ccs1Δ* as being hypersensitive to PAF. Ccs1p is a copper chaperon needed for yeast superoxide dismutase (*SOD1*) function (143). This suggests that the power of chemical genomics in yeast can be utilized to study PAF effects including but not limited to neurodegeneration.

In rat brain injury models, L-Carnitine preincubation has been shown to reduce endogenous PAF concentrations. This suggested that L-Carnitine has a neuroprotective

effect and that reduced levels of L-Carnitine can lead to higher PAF levels (144). My results have yielded insights into this process as well. *AGP2*, a plasma membrane carnitine transporter was identified in my screen. Interestingly, carnitine uptake is regulated by the HOG pathway and I identified a gene that regulates the HOG pathway in my screens (*SHO1*). The HOG pathway is involved in osmotic sensing and adjustment. Sho1p detects high osmolarity on the cell surface and affects downstream MAP kinases (145). It was found that osmotic stress leads to decreased carnitine uptake via the Sho1p-mediated activation of Hog1p which suppresses the expression of *AGP2* (145). These results implicate PAF in yeast to the carnitine uptake and osmosensing pathways.

4.3 Actin And Spindle Effects of PAF Treatment

Interestingly my screens identified 13 deletion mutants whose genes encode proteins with defined roles in cytoskeleton and implicated PAF in impacting the actin cytoskeleton. In agreement with this, I observed in one experiment that PAF-treatment causes actin disruption. This lead to spindle misorientation and binucleate cells (Figures 11, 12, and 13). As actin depolymerization/disruption can cause cell cycle arrest (146) the PAF-dependent disruption of the actin cytoskeleton may be responsible for the observed PAF cell cycle arrest. However, the actin experiment was performed once and will need to be replicated. PAF-treatment causes similar effects on the cytoskeleton in mammalian cells. For example, when neutrophils are stimulated with PAF they undergo an actin response that is characterized by three stages: an initial polymerization event, then a rapid oscillation between polymerization/depolymerization, followed with a gradual depolymerization to initial basal levels (64). These effects are thought to occur due to an intracellular signalling mechanism dependant on PKC and myosin phosphorylation (64).

L-PAF on the other hand did not exhibit actin polymerization effects (65). Whether these effects occur through the PAF receptor remains unclear (64, 65). Also, PAF induced clathrin-mediated endocytosis, cell polarization, and actin bundle formation at the site of PAFR in neutrophils (147). My results (Figures 11, 12, and 13) parallel those obtained in mammalian studies of PAF and suggest a conservation of the mechanism of action. In yeast, clathrin is found at the cortical actin patches (148) the sites of actin cable assembly (reviewed in 51). Hence, one could hypothesize that PAF may be causing its effects through clathrin disruption which would lead to defective patches and thus less actin cables.

The high rate of binucleate cells and spindle misorientation may be indicative of PAF-dependent effects on actin cables (53). The Kar9 and Dynein pathways are parallel pathways involved in orienting the spindle such that the loss of both is lethal (55). The spindle orient by attaching astral microtubules to actin cables extending from the bud (reviewed in 56). In the Dynein pathway, the dynactin complex localizes to the ends of astral microtubules and pulls the spindle through the bud neck. This complex is required for dynein activity (55). On the other hand, a complex composed of Bim1p, Kar9p, and Myo2p attaches the astral microtubules to the actin cables and orients the spindle (reviewed in 57). Mutants of the dynactin complex have spindle orientation defects and it is interesting to note that *LDB18* (human p24), which is required for dynactin integrity (55), was identified in my chemical-genetic screen. As chemical-genetic screens provide synthetic-chemical interactions that predict function, it suggests that PAF may be affecting the parallel Kar9 pathway. An alternate explanation would be that the effect of

PAF on actin cables is exacerbated in mutants that have problems attaching the spindle to actin as would be seen in mutants that affect dynactin integrity.

In yeast, there are two major spindle position checkpoint proteins (*BUB2* and *BFA1*) (reviewed in 149). These two proteins block the cell cycle until the spindle is oriented in the mother-bud axis. One of the hits in the haploinsufficiency screen was a spindle checkpoint mutant, *IBD2*, which plays it role upstream of these two checkpoint controlling proteins and displays spindle orientation defects upon deletion (58). This leads me to believe that PAF is not directly causing a spindle orientation defect but rather this defect is a consequence of PAF's effect on actin cables. This effect is then exacerbated in spindle orientation defective mutants making it seem as though PAF is directly acting on the spindle.

All of the above leads me to conclude that PAF's effects on the cytoskeleton are multifaceted and not limited to one pathway. The microtubules, the cables, and the patches are all affected either on the level of assembly or at a regulatory level. These results parallel those obtained in mammalian studies and suggest a conservation of the mechanism of PAF action between man and yeast.

4.4 YDL133W

The ability of the chemical genomic screens to identify relevant proteins/pathways implicated in PAF action, suggests that not only is the screen successfully but that it may also provide unique insights into PAF mode-of-action. As I am interested in C16:0 PAF-dependent neurotoxicity, I was particularly interested in mutants that displayed hypersensitivity to C16:0PAF only. Remarkably *ydl133wΔ* cells were highly sensitive to C16:0 PAF treatment, yet displayed no L-PAF sensitivity beyond

wildtype (Figure 14). As well it was one of only three mutants identified in both the haploid and diploid screens. The other two mutants identified were *spo14Δ* and *sct1Δ* which both have direct roles in PAF metabolism in yeast (99), hence it suggests that Ydl133w has a pivotal role in mediating PAF signalling in yeast.

Very little is known about Ydl133wp. It is predicted to be a four trans- membrane domain protein, however its cellular localization has not been determined. Ydl133wp is needed for calcium influx during mating (133), and *YDL133w* expression is induced upon mating factor treatment (150). This suggests that Ydl133w plays an important role in Calcium influx during times of polarization of the cytoskeleton, such as mating protrusion, by a yet to be determine molecular mechanism. Intriguingly, a high-throughput chemical genomic screen which examined 1144 compounds and environmental conditions, suggested that *YDL133w* has a co-fitness phenotype with *ENT1* (131). Co-fitness was defined as the correlation of the profiles across all the conditions tested and provides a prediction of function. Ent1p is a protein that binds clathrin and is involved in endocytosis and actin patch assembly. Further, my SL-SGA screen determined that five out of the 15 deletion mutants that display synthetic sick/lethal interactions with *ydl133wΔ* are involved in vesicle mediated transport and endocytosis (Table 3). These interactions suggest that Ydl133wp may play a role in vesicle transport or endocytosis. One intriguing possibility is that Ydl133wp maybe regulating Ca2+ fluxes which in turn regulate actin cytoskeleton remodelling and transport that is imperative during periods of polarized growth such as mating. Unfortunately attempts at localizing Ydl133wp or discerning its proteins interactions failed, hence though central to the PAF response in yeast, its cellular function remains

elusive. To fully dissect yeast's cellular response to PAF will require the careful characterization of Ydl133wp.

4.5 Final Conclusions

The objective of this study was to determine if yeast is a useful model for dissecting C16:0 PAF-dependent neuronal cell death and exploit the systematic mutant screens available in yeast to determine novel PAF mode-of-action. I determined that that yeast and mammalians cells are toxic to C16:0 PAF but not L-PAF, and importantly numerous cellular effects of PAF treatment are conserved, including G1 cell cycle arrest and depolarization of the actin cytoskeleton. This suggests that yeast is a potentially usefully model for PAF-receptor independent toxicity. Importantly, my chemical genomic screens do not only identify known mutants with sensitivity to PAF, but identify known biological pathways/processes affected by PAF treatment. This strongly argues that not only are PAF-dependent signalling modules conserved, but that the screens will provide a wealth of novel predictions as to the mode-of-action of PAF *in vivo*.

4.6 Future Directions

Previous studies on wildtype yeast have shown it to be sensitive to PAF in liquid media (94) and to both PAF and L-PAF on solid media (99) In my experiments have seen some strains that were sensitive to both compounds on solid media but only to PAF in liquid media. In order to resolve the discrepancy seen in liquid versus solid media I propose two experiments. First, test another medium having different ingredients such as minimal media. Second, perform dot assays to re-confirm all the putative hits on solid media as opposed to the quantitative growth curves I performed in 96-well plates. C16:0

L-PAF was chosen as a control lipid because it did not elicit neuronal cell death (11). Other beneficial control lipids could be PAF-like lipids and C18:0 species. PAF-like species tend to have decreasing bioactivity with increasing chain length at the sn-2 position (151). Also, C18:0 PAF and C18:0 L-PAF have apoptotic effects in neurons that are though different signalling pathways than C16:0 PAF (60).

The preliminary Lipidomics profiling can be improved by the following: First, three replicas are needed (haploid and diploid). Second, some controls must be added to solidify the interpretation. For example, some samples will require the addition of PAF-AH as a positive control to show that PAF does not degrade in yeast cells except when PAF-AH is added. Also, an *ALE1* deletion mutant should be analyzed to provide evidence that L-PAF is truly being acetylated to make PAF in yeast. An internal standard (for absolute quantitation and enhanced normalization) should be added prior to sample injection into the mass spectrometric. Finally, the methodology must be optimized such that the washes during the lipid extraction are done with BSA instead of YPD (to keep the media separate from the cells). This data can be complemented with a fluorescently labelled PAF (bodipy-PAF) to show PAF entering the cells. Further, a protein called Lem3p is needed for the uptake of edelfosine and would serve as a good secondary control to test if PAF is entering the cells (105, 107). Whether PAF enters the cells by endocytosis (suggested by *CLC1*) can be tested using *end4* deletion strains that block endocytosis.

Finally, I suggest other experiments that would complement my current work. First, the cell cycle results can be complemented with propidium-iodide staining followed by flow cytometry analysis. Second, instead of using CFU to detect cell death one can

analyze the levels of reactive oxygen species by the addition of H_2DCF-DA, TUNEL staining to show DNA breakage, propidium-iodide staining followed by flow cytometry to see degraded DNA, cell staining with Phloxin B dye which accumulates in dead cells, and methylene blue staining (107, 135). Third, perform an overexpression screen on PAF. Fourth, check if addition of carnitine or SOD to the growth curves along with PAF has an alleviating effect. Finally, characterize *YDL133w* function using calcium influx assays (152).

REFERENCE LIST

1. Sweet, R.A., K. Panchalingam, J.W. Pettegrew, R.J. McClure, R.L. Hamilton, O.L. Lopez, D.I. Kaufer, S.T. DeKosky, and W.E. Klunk. 2002. Psychosis in Alzheimer disease: Postmortem magnetic resonance spectroscopy evidence of excess neuronal and membrane phospholipid pathology. *Neurobiology of Aging* 23:547-553.
2. Klunk, W.E., C.J. Xu, R.J. McClure, K. Panchalingam, J.A. Stanley, and J.W. Pettegrew. 1997. Aggregation of Î²-amyloid peptide is promoted by membrane phospholipid metabolites elevated in Alzheimer's disease brain. *Journal of Neurochemistry* 69:266-272.
3. Kanfer, J.N., G. Sorrentino, and D.S. Sitar. 1998. Phospholipases as mediators of amyloid beta peptide neurotoxicity: An early event contributing to neurodegeneration characteristic of Alzheimer's disease. *Neuroscience Letters* 257:93-96.
4. Klein, J. 2000. Membrane breakdown in acute and chronic neurodegeneration: Focus on choline-containing phospholipids. *Journal of Neural Transmission* 107:1027-1063.
5. Bate, C., M. Salmona, and A. Williams. 2004. The role of platelet activating factor in prion and amyloid-Î² neurotoxicity. *NeuroReport* 15:509-513.
6. Farooqui, A.A., W.Y. Ong, and L.A. Horrocks. 2004. Biochemical aspects of neurodegeneration in human brain: Involvement of neural membrane phospholipids and phospholipases A2. *Neurochemical Research* 29:1961-1977.
7. Bellizzi, M.J., S.M. Lu, E. Masliah, and H.A. Gelbard. 2005. Synaptic activity becomes excitotoxic in neurons exposed to elevated levels of platelet-activating factor. *Journal of Clinical Investigation* 115:3185-3192.
8. Bennett, S.A.L., J. Chen, B.A. Pappas, D.C.S. Roberts, and M. Tenniswood. 1998. Platelet activating factor receptor expression is associated with neuronal apoptosis in an in vivo model of excitotoxicity. *Cell Death and Differentiation* 5:867-875.
9. Tong, N., J.F. Sanchez, S.B. Maggirwar, S.H. Ramirez, H. Guo, S. Dewhurst, and H.A. Gelbard. 2001. Activation of glycogen synthase kinase 3 beta (GSK-3Î²) by platelet activating factor mediates migration and cell death in cerebellar granule neurons. *European Journal of Neuroscience* 13:1913-1922.
10. Xu, Y., B. Zhang, Z. Hua, R.A. Johns, D.S. Bredt, and Y.X. Tao. 2004. Targeted disruption of PSD-93 gene reduces platelet-activating factor-induced neurotoxicity in cultured cortical neurons. *Experimental Neurology* 189:16-24.
11. Ryan, S.D., C.S. Harris, F. Mo, H. Lee, S.T. Hou, N.G. Bazan, P.S. Haddad, J.T. Arnason, and S.A.L. Bennett. 2007. Platelet activating factor-induced neuronal apoptosis is initiated independently of its G-protein coupled PAF receptor and is inhibited by the benzoate orsellinic acid. *Journal of Neurochemistry* 103:88-97.

12. Bach, S., N. Talarek, T. Andrieu, J.M. Vierfond, Y. Mettey, H. Galons, D. Dormont, L. Meijer, C. Cullin, and M. Blondel. 2003. Isolation of drugs active against mammalian prions using a yeast-based screening assay. *Nature Biotechnology* 21:1075-1081.
13. Bach, S., D. Tribouillard, N. Talarek, N. Desban, F. Gug, H. Galons, and M. Blondel. 2006. A yeast-based assay to isolate drugs active against mammalian prions. *Methods* 39:72-77.
14. Feng, B.Y., B.H. Toyama, H. Wille, D.W. Colby, S.R. Collins, B.C.H. May, S.B. Prusiner, J. Weissman, and B.K. Shoichet. 2008. Small-molecule aggregates inhibit amyloid polymerization. *Nature Chemical Biology* 4:197-199.
15. Middendorp, O., C. Ortler, U. Neumann, P. Paganetti, U. LuÌˆthi, and A. Barberis. 2004. Yeast growth selection system for the identification of cell-active inhibitors of Î²-secretase. *Biochimica et Biophysica Acta - General Subjects* 1674:29-39.
16. Outeiro, T.F., and S. Lindquist. 2003. Yeast Cells Provide Insight into Alpha-Synuclein Biology and Pathobiology. *Science* 302:1772-1775.
17. Willingham, S., T.F. Outeiro, M.J. DeVit, S.L. Lindquist, and P.J. Muchowski. 2003. Yeast Genes that Enhance the Toxicity of a Mutant Huntingtin Fragment or Î±-Synuclein. *Science* 302:1769-1772.
18. Zhang, W., D. Espinoza, V. Hines, M. Innis, P. Mehta, and D.L. Miller. 1997. Characterization of Î²-amyloid peptide precursor processing by the yeast Yap3 and Mkc7 proteases. *Biochimica et Biophysica Acta - Molecular Cell Research* 1359:110-122.
19. Bowers, K., and T.H. Stevens. 2005. Protein transport from the late Golgi to the vacuole in the yeast Saccharomyces cerevisiae. *Biochimica et Biophysica Acta - Molecular Cell Research* 1744:438-454.
20. Korolev, V.G. 2007. Molecular mechanisms of double strand break repair in eukaryotes. *Radiatsionnaia biologiia, radioecologiia / Rossii?skaia akademiia nauk* 47:389-401.
21. Barr, F.A., and U. Gruneberg. 2007. Cytokinesis: Placing and Making the Final Cut. *Cell* 131:847-860.
22. Sclafani, R.A., and T.M. Holzen. 2007. Cell cycle regulation of DNA replication. *Annual review of genetics* 41:237-280.
23. Niwa, M. 2006. The unfolded protein response unfolds. *Topics in Current Genetics* 16:35-63.
24. Sychrova, H. 2004. Yeast as a Model Organism to Study Transport and Homeostasis of Alkali Metal Cations. *Physiological Research* 53:S91-S98.
25. Sherman, F. 2002. Getting started with yeast. *Methods in Enzymology* 350:3-41.
26. Cherry, J.M., C. Ball, S. Weng, G. Juvik, R. Schmidt, C. Adler, B. Dunn, S. Dwight, L. Riles, R.K. Mortimer, and D. Botstein. 1997. Genetic and physical maps of Saccharomyces cerevisiae. *Nature* 387:67-73.
27. Fisk, D.G., C.A. Ball, K. Dolinski, S.R. Engel, E.L. Hong, L. Issel-Tarver, K. Schwartz, A. Sethuraman, D. Botstein, and J.M. Cherry. 2006. Saccharomyces cerevisiae S288C genome annotation: A working hypothesis. *Yeast* 23:857-865.
28. Dolinski, K., and D. Botstein. 2005. Changing perspectives in yeast research nearly a decade after the genome sequence. *Genome Research* 15:1611-1619.

29. Zhu, H., M. Bilgin, R. Bangham, D. Hall, A. Casamayor, P. Bertone, N. Lan, R. Jansen, S. Bidlingmaier, T. Houfek, T. Mitchell, P. Miller, R.A. Dean, M. Gerstein, and M. Snyder. 2001. Global analysis of protein activities using proteome chips. *Science* 293:2101-2105.
30. Winzeler, E.A., D.D. Shoemaker, A. Astromoff, H. Liang, K. Anderson, B. Andre, R. Bangham, R. Benito, J.D. Boeke, H. Bussey, A.M. Chu, C. Connelly, K. Davis, F. Dietrich, S.W. Dow, M. El Bakkoury, F. Foury, S.H. Friend, E. Gentalen, G. Giaever, J.H. Hegemann, T. Jones, M. Laub, H. Liao, N. Liebundguth, D.J. Lockhart, A. Lucau-Danila, M. Lussier, N. M'Rabet, P. Menard, M. Mittmann, C. Pai, C. Rebischung, J.L. Revuelta, L. Riles, C.J. Roberts, P. Ross-MacDonald, B. Scherens, M. Snyder, S. Sookhai-Mahadeo, R.K. Storms, S. Veì□ronneau, M. Voet, G. Volckaert, T.R. Ward, R. Wysocki, G.S. Yen, K. Yu, K. Zimmermann, P. Philippsen, M. Johnston, and R.W. Davis. 1999. Functional characterization of the S. cerevisiae genome by gene deletion and parallel analysis. *Science* 285:901-906.
31. Bassett Jr, D.E., M.S. Boguski, and P. Hieter. 1996. Yeast genes and human disease [2]. *Nature* 379:589-590.
32. Foury, F. 1997. Human genetic diseases: A cross-talk between man and yeast. *Gene* 195:1-10.
33. Perocchi, F., E. Mancera, and L.M. Steinmetz. 2007. Systematic screens for human disease genes, from yeast to human and back. *Molecular BioSystems* 4:18-29.
34. Steinmetz, L.M., C. Scharfe, A.M. Deutschbauer, D. Mokranjac, Z.S. Herman, T. Jones, A.M. Chu, G. Giaever, H. Prokisch, P.J. Oefner, and R.W. Davis. 2002. Systematic screen for human disease genes in yeast. *Nature Genetics* 31:400-404.
35. Hartwell, L., T. Weinert, L. Kadyk, and B. Garvik. 1994. Cell cycle checkpoints, genomic integrity, and cancer. *Cold Spring Harbor Symposia on Quantitative Biology* 59:259-263.
36. Weinert, T. 1997. Yeast checkpoint controls and relevance to cancer. *Cancer Surveys* 29:109-132.
37. Esler, W.P., and M.S. Wolfe. 2001. A portrait of Alzheimer secretases - New features and familiar faces. *Science* 293:1449-1454.
38. Luì^cking, C.B., and A. Brice. 2000. Alpha-synuclein and Parkinson's disease. *Cellular and Molecular Life Sciences* 57:1894-1908.
39. Cooper, A.A., A.D. Gitler, A. Cashikar, C.M. Haynes, K.J. Hill, B. Bhullar, K. Liu, K. Xu, K.E. Strathearn, F. Liu, S. Cao, K.A. Caldwell, G.A. Caldwell, G. Marsischky, R.D. Kolodner, J. LaBaer, J.C. Rochet, N.M. Bonini, and S. Lindquist. 2006. Î±-synuclein blocks ER-Golgi traffic and Rab1 rescues neuron loss in Parkinson's models. *Science* 313:324-328.
40. Tong, A.H.Y., M. Evangelista, A.B. Parsons, H. Xu, G.D. Bader, N. Pageì□, M. Robinson, S. Raghibizadeh, C.W.V. Hogue, H. Bussey, B. Andrews, M. Tyers, and C. Boone. 2001. Systematic genetic analysis with ordered arrays of yeast deletion mutants. *Science* 294:2364-2368.
41. Giorgini, F., P. Guidetti, Q. Nguyen, S.C. Bennett, and P.J. Muchowski. 2005. A genomic screen in yeast implicates kynurenine 3-monooxygenase as a therapeutic target for Huntington disease. *Nature Genetics* 37:526-531.

42. MacDonald, M.E., C.M. Ambrose, M.P. Duyao, R.H. Myers, C. Lin, L. Srinidhi, G. Barnes, S.A. Taylor, M. James, N. Groot, H. MacFarlane, B. Jenkins, M.A. Anderson, N.S. Wexler, J.F. Gusella, G.P. Bates, S. Baxendale, H. Hummerich, S. Kirby, M. North, S. Youngman, R. Mott, G. Zehetner, Z. Sedlacek, A. Poustka, A.-M. Frischauf, H. Lehrach, A.J. Buckler, D. Church, L. Doucette-Stamm, M.C. O'Donovan, L. Riba-Ramirez, M. Shah, V.P. Stanton, S.A. Strobel, K.M. Draths, J.L. Wales, P. Dervan, D.E. Housman, M. Altherr, R. Shiang, L. Thompson, T. Fielder, J.J. Wasmuth, D. Tagle, J. Valdes, L. Elmer, M. Allard, L. Castilla, M. Swaroop, K. Blanchard, F.S. Collins, R. Snell, T. Holloway, K. Gillespie, N. Datson, D. Shaw, and P.S. Harper. 1993. A novel gene containing a trinucleotide repeat that is expanded and unstable on Huntington's disease chromosomes. *Cell* 72:971-983.
43. Nasir, J., S.B. Floresco, J.R. O'Kusky, V.M. Diewert, J.M. Richman, J. Zeisler, A. Borowski, J.D. Marth, A.G. Phillips, and M.R. Hayden. 1995. Targeted disruption of the Huntington's disease gene results in embryonic lethality and behavioral and morphological changes in heterozygotes. *Cell* 81:811-823.
44. Fernandis, A.Z., and M.R. Wenk. 2007. Membrane lipids as signaling molecules. *Current Opinion in Lipidology* 18:121-128.
45. Ivanova, P.T., S.B. Milne, M.O. Byrne, Y. Xiang, and H.A. Brown. 2007. Glycerophospholipid identification and quantitation by electrospray ionization mass spectrometry. *Methods in enzymology* 432:21-57.
46. Prescott, S.M., G.A. Zimmerman, D.M. Stafforini, and T.M. McIntyre. 2000. Platelet-activating factor and related lipid mediators. *Annual Review of Biochemistry* 69:419-445.
47. Exton, J.H. 1994. Messenger molecules derived from membrane lipids. *Current Opinion in Cell Biology* 6:226-229.
48. Goto, K., Y. Hozumi, T. Nakano, S. Saino-Saito, and A.M. Martelli. 2008. Lipid messenger, diacylglycerol, and its regulator, diacylglycerol kinase, in cells, organs, and animals: History and perspective. *Tohoku Journal of Experimental Medicine* 214:199-212.
49. Irvine, R.F. 1992. Inositol lipids in cell signalling. *Current Opinion in Cell Biology* 4:212-219.
50. English, D., Y. Cui, and R.A. Siddiqui. 1996. Messenger functions of phosphatidic acid. *Chemistry and Physics of Lipids* 80:117-132.
51. Moseley, J.B., and B.L. Goode. 2006. The yeast actin cytoskeleton: From cellular function to biochemical mechanism. *Microbiology and Molecular Biology Reviews* 70:605-645.
52. Young, M., J. Cooper, and P. Bridgman. 2004. Yeast actin patches are networks of branched actin filaments. *Journal of Cell Biology* 166:629–635.
53. Palmer, R.E., D.S. Sullivan, T. Huffaker, and D. Koshland. 1992. Role of astral microtubules and actin in spindle orientation and migration in the budding yeast, Saccharomyces cerevisiae. *Journal of Cell Biology* 119:583-594.
54. Fraschini, R., M. Venturetti, E. Chiroli, and S. Piatti. 2008. The spindle position checkpoint: How to deal with spindle misalignment during asymmetric cell division in budding yeast. *Biochemical Society Transactions* 36:416-420.

55. Amaro, I.A., M. Costanzo, C. Boone, and T.C. Huffaker. 2008. The Saccharomyces cerevisiae homolog of p24 is essential for maintaining the association of p150Glued with the dynactin complex. *Genetics* 178:703-709.
56. Segal, M., and K. Bloom. 2001. Control of spindle polarity and orientation in Saccharomyces cerevisiae. *Trends in Cell Biology* 11:160-166.
57. Schuyler, S.C., and D. Pellman. 2001. Search, capture and signal: Games microtubules and centrosomes play. *Journal of Cell Science* 114:247-255.
58. Hwang, H.S., and K. Song. 2002. IBD2 encodes a novel component of the Bub2p-dependent spindle checkpoint in the budding yeast Saccharomyces cerevisiae. *Genetics* 161:595-609.
59. Benveniste, J., P.M. Henson, and C.G. Cochrane. 1972. Leukocyte-dependent histamine release from rabbit platelets. The role of IgE, basophils, and a platelet-activating factor. *Journal of Experimental Medicine* 136:1356-1377.
60. Ryan, S.D., C.S. Harris, C.L. Carswell, J.E. Baenziger, and S.A. Bennett. 2008. Heterogeneity in the sn-1 carbon chain of platelet activating factor glycerophospholipids determines pro-or anti-apoptotic signaling in primary neurons. *Journal of Lipid Research*
61. Ishii, S., and T. Shimizu. 2000. Platelet-activating factor (PAF) receptor and genetically engineered PAF receptor mutant mice. *Progress in Lipid Research* 39:41-82.
62. Ishii, S., T. Nagase, F. Tashiro, K. Ikuta, S. Sato, I. Waga, K. Kume, J.I. Miyazaki, and T. Shimizu. 1997. Bronchial hyperreactivity, increased endotoxin lethality and melanocytic tumorigenesis in transgenic mice overexpressing platelet-activating factor receptor. *EMBO Journal* 16:133-142.
63. Fukuda, Y., H. Kawashima, K. Saito, N. Inomata, M. Matsui, and T. Nakanishi. 2000. Effect of human plasma-type platelet-activating factor acetylhydrolase in two anaphylactic shock models. *European Journal of Pharmacology* 390:203-207.
64. Rengan, R., and G.M. Omann. 1999. Regulation of oscillations in filamentous actin content in polymorphonuclear leukocytes stimulated with leukotriene B4 and platelet-activating factor. *Biochemical and Biophysical Research Communications* 262:479-486.
65. Shalit, M., G.A. Dabiri, and F.S. Southwick. 1987. Platelet-activating factor both stimulates and 'primes' human polymorphonuclear leukocyte actin filament assembly. *Blood* 70:1921-1927.
66. Ebisawa, M., H. Saito, and Y. Iikura. 1990. Platelet-activating factor-induced activation and cytoskeletal change in cultured eosinophils. *International Archives of Allergy and Applied Immunology* 93:93-98.
67. Kume, K., and T. Shimizu. 1997. Platelet-activating Factor (PAF) Induces Growth Stimulation, Inhibition, and Suppression of Oncogenic Transformation in NRK Cells Overexpressing the PAF Receptor. *Journal of Biological Chemistry* 272:22898-22904.
68. Behrens, T.W., and J.S. Goodwin. 1990. Control of human T cell proliferation by platelet-activating factor. *International Journal of Immunopharmacology* 12:175-184.

69. Roth, M., M. Nauck, S. Yousefi, M. Tamm, K. Blaser, A.P. Perruchoud, and H.U. Simon. 1996. Platelet-activating factor exerts mitogenic activity and stimulates expression of interleukin 6 and interleukin 8 in human lung fibroblasts via binding to its functional receptor. *Journal of Experimental Medicine* 184:191-201.
70. Chen, C., and N.G. Bazan. 2005. Lipid signaling: Sleep, synaptic plasticity, and neuroprotection. *Prostaglandins and Other Lipid Mediators* 77:65-76.
71. Heusler, P., and G. Boehmer. 2007. Platelet-activating factor contributes to the induction of long-term potentiation in the rat somatosensory cortex in vitro. *Brain Research* 1135:85-91.
72. Chen, C., J.C. Magee, V. Marcheselli, M. Hardy, and N.G. Bazan. 2001. Attenuated LTP in hippocampal dentate gyrus neurons of mice deficient in the PAF receptor. *Journal of Neurophysiology* 85:384-390.
73. Perry, S.W., J.A. Hamilton, L.W. Tjoelker, G. Dbaibo, K.A. Dzenko, L.G. Epstein, Y. Hannun, J. Steven Whittaker, S. Dewhurst, and H.A. Gelbard. 1998. Platelet-activating factor receptor activation. An initiator step in HIV-1 neuropathogenesis. *Journal of Biological Chemistry* 273:17660-17664.
74. Bazan, N.G. 1998. The neuromessenger platelet-activating factor in plasticity and neurodegeneration. *Progress in Brain Research* 118:281-291.
75. Bazan, N.G., B. Tu, and E.B. Rodriguez de Turco. 2002. What synaptic lipid signaling tells us about seizure-induced damage and epileptogenesis. In Progress in Brain Research. 175-185.
76. Farooqui, A.A., W.Y. Ong, and L.A. Horrocks. 2006. Inhibitors of brain phospholipase A2 activity: Their neuropharmacological effects and therapeutic importance for the treatment of neurologic disorders. *Pharmacological Reviews* 58:591-620.
77. Li, T., M.D. Southall, Q. Yi, Y. Pei, D. Lewis, M. Al-Hassani, D. Spandau, and J.B. Travers. 2003. The epidermal platelet-activating factor receptor augments chemotherapy-induced apoptosis in human carcinoma cell lines. *Journal of Biological Chemistry* 278:16614-16621.
78. Darst, M., M. Al-Hassani, T. Li, Q. Yi, J.M. Travers, D.A. Lewis, and J.B. Travers. 2004. Augmentation of Chemotherapy-Induced Cytokine Production by Expression of the Platelet-Activating Factor Receptor in a Human Epithelial Carcinoma Cell Line. *Journal of Immunology* 172:6330-6335.
79. Igbavboa, U., J. Hamilton, H.Y. Kim, G.Y. Sun, and W.G. Wood. 2002. A new role for apolipoprotein E: Modulating transport of polyunsaturated phospholipid molecular species in synaptic plasma membranes. *Journal of Neurochemistry* 80:255-261.
80. Brewer, C., F. Bonin, P. Bullock, M.C. Nault, J. Morin, S. Imbeault, T.Y. Shen, D.J. Franks, and S.A.L. Bennett. 2002. Platelet activating factor-induced apoptosis is inhibited by ectopic expression of the platelet activating factor G-protein coupled receptor. *Journal of Neurochemistry* 82:1502-1511.
81. Shindou, H., D. Hishikawa, H. Nakanishi, T. Harayama, S. Ishii, R. Taguchi, and T. Shimizu. 2007. A single enzyme catalyzes both platelet-activating factor production and membrane biogenesis of inflammatory cells: Cloning and characterization of acetyl-CoA:lyso-PAF acetyltransferase. *Journal of Biological Chemistry* 282:6532-6539.

82. Leslie, C.C. 2004. Regulation of the specific release of arachidonic acid by cytosolic phospholipase A2. *Prostaglandins Leukotrienes and Essential Fatty Acids* 70:373-376.
83. Tamaki, H., A. Shimada, Y. Ito, M. Ohya, J. Takase, M. Miyashita, H. Miyagawa, H. Nozaki, R. Nakayama, and H. Kumagai. 2007. LPT1 encodes a membrane-bound O-acyltransferase involved in the acylation of lysophospholipids in the yeast Saccharomyces cerevisiae. *Journal of Biological Chemistry* 282:34288-34298.
84. Snyder, F., T.C. Lee, and M.L. Blank. 1992. The role of transacylases in the metabolism of arachidonate and platelet activating factor. *Progress in Lipid Research* 31:65-86.
85. Kawasaki, T., and F. Snyder. 1987. The metabolism of lyso-platelet-activating factor (1-O-alkyl-2-lyso-sn-glycero-3-phosphocholine) by a calcium-dependent lysophospholipase D in rabbit kidney medulla. *Biochimica et Biophysica Acta (BBA)/Lipids and Lipid Metabolism* 920:85-93.
86. Snyder, F. 1995. Platelet-activating fator and its analogs: Metabolic pathways and related intracellular processes. *Biochimica et Biophysica Acta - Lipids and Lipid Metabolism* 1254:231-249.
87. Tanaka, T., H. Minamino, S. Unezaki, H. Tsukatani, and A. Tokumura. 1993. Formation of platelet-activating factor-like phospholipids by Fe2+/ascorbate/EDTA-induced lipid peroxidation. *Biochimica et Biophysica Acta - Lipids and Lipid Metabolism* 1166:264-274.
88. Itabe, H., Y. Kushi, S. Handa, and K. Inoue. 1988. Identification of 2-azelaoylphosphatidylcholine as one of the cytotoxic products generated during oxyhemoglobin-induced peroxidation of phosphatidylcholine. *Biochimica et Biophysica Acta - Lipids and Lipid Metabolism* 962:8-15.
89. Peplow, P.V. 1999. Regulation of platelet-activating factor (PAF) activity in human diseases by phospholipase A2 inhibitors, PAF acetylhydrolases, PAF receptor antagonists and free radical scavengers. *Prostaglandins Leukotrienes and Essential Fatty Acids* 61:65-82.
90. Rola-Pleszczynski, M., M. Thivierge, S. Ouellet, P. Dagenais, J.L. Parent, and J. Stankova. 1995. Cytokines and eicosanoids regulate PAF receptor gene expression. *Advances in prostaglandin, thromboxane, and leukotriene research* 23:287-292.
91. Nakayama, R., H. Kumagai, and K. Saito. 1994. Evidence for production of platelet-activating factor by yeast Saccharomyces cerevisiae cells. *Biochimica et Biophysica Acta - General Subjects* 1199:137-142.
92. Roudebush, W.E., R.J. Straˆub, J.B. Massey, and H.I. Kort. 2006. Temporal production of platelet-activating factor by Brewer's yeast. *Journal of the American Society of Brewing Chemists* 64:135-138.
93. Nakayama, R., H. Udagawa, and H. Kumagai. 1997. Changes in PAF (platelet-activating factor) production during cell cycle of yeast Saccharomyces cerevisiae. *Bioscience, Biotechnology and Biochemistry* 61:631-635.
94. Nakayama, R., C. Yun, H. Tamaki, K. Saito, and H. Kumagai. 1997. Physiological action of PAF in yeast Saccharomyces cerevisiae. *Advances in Experimental Medicine and Biology* 416:45-50.

95. Foulks, J.M., A.S. Weyrich, G.A. Zimmerman, and T.M. McIntyre. 2008. A yeast PAF acetylhydrolase ortholog suppresses oxidative death. *Free Radical Biology and Medicine* 45:434-442.
96. Jain, S., N. Stanford, N. Bhagwat, B. Seiler, M. Costanzo, C. Boone, and P. Oelkers. 2007. Identification of a novel lysophospholipid acyltransferase in Saccharomyces cerevisiae. *Journal of Biological Chemistry* 282:30562-30569.
97. Richard, M.G., and C.R. McMaster. 1998. Lysophosphatidylcholine acyltransferase activity in Saccharomyces cerevisiae: Regulation by a high-affinity Zn2+ binding site. *Lipids* 33:1229-1234.
98. Huh, W.K., J.V. Falvo, L.C. Gerke, A.S. Carroll, R.W. Howson, J.S. Weissman, and E.K. O'Shea. 2003. Global analysis of protein localization in budding yeast. *Nature* 425:686-691.
99. Zaremberg, V., and C.R. McMaster. 2002. Differential partitioning of lipids metabolized by separate yeast glycerol-3-phosphate acyltransferases reveals that phospholipase D generation of phosphatidic acid mediates sensitivity to choline-containing lysolipids and drugs. *Journal of Biological Chemistry* 277:39035-39044.
100. Lichko, L.P., T.V. Kulakovskaia, and I.S. Kulaev. 1994. The effect of PAF, sphingosine and heparin on certain phosphohydrolase and transport activity of yeast vacuoles. *Biokhimiya* 59:1088-1097.
101. Fyrst, H., B. Oskouian, F.A. Kuypers, and J.D. Saba. 1999. The PLB2 gene of Saccharomyces cerevisiae confers resistance to lysophosphatidylcholine and encodes a phospholipase B/lysophospholipase. *Biochemistry* 38:5864-5871.
102. Merkel, O., M. Fido, J.A. Mayr, H. Pru?ger, F. Raab, G. Zandonella, S.D. Kohlwein, and F. Paltauf. 1999. Characterization and function in vivo of two novel phospholipases B/lysophospholipases from Saccharomyces cerevisiae. *Journal of Biological Chemistry* 274:28121-28127.
103. Patterson, M.C. 2003. A Riddle Wrapped in a Mystery: Understanding Niemann-Pick Disease, Type C. *Neurologist* 9:301-310.
104. Pentchev, P.G., M.E. Comly, and H.S. Kruth. 1985. A defect in cholesterol esterification in Niemann-Pick disease (type C) patients. *Proceedings of the National Academy of Sciences of the United States of America* 82:8247-8251.
105. Berger, A.C., P.K. Hanson, J.W. Nichols, and A.H. Corbett. 2005. A yeast model system for functional analysis of the Niemann-Pick type C protein 1 homolog, Ncr1p. *Traffic* 6:907-917.
106. Zhang, H., C. Gajate, L.-p. Yu, Y.-x. Fang, and F. Mollinedo. 2007. Mitochondrial-derived ROS in edelfosine-induced apoptosis in yeasts and tumor cells. *Acta Pharmacologica Sinica* 28:888-894.
107. Hanson, P.K., L. Malone, J.L. Birchmore, and J.W. Nichols. 2003. Lem3p is essential for the uptake and potency of alkylphosphocholine drugs, edelfosine and miltefosine. *Journal of Biological Chemistry* 278:36041-36050.
108. Zaremberg, V., C. Gajate, L.M. Cacharro, F. Mollinedo, and C.R. McMaster. 2005. Cytotoxicity of an anti-cancer lysophospholipid through selective modification of lipid raft composition. *Journal of Biological Chemistry* 280:38047-38058.

109. Sauer, U., M. Heinemann, and N. Zamboni. 2007. GENETICS: Getting Closer to the Whole Picture. *Science* 316:550-551.
110. Westont, A.D., and L. Hood. 2004. Systems Biology, Proteomics, and the Future of Health Care: Toward Predictive, Preventative, and Personalized Medicine. *Journal of Proteome Research* 3:179-196.
111. Kitano, H. 2002. Computational Systems Biology. *Nature* 420:206-210.
112. Kitano, H. 2002. Systems Biology: A Brief Overview. *Science* 295:1662-1664.
113. Mustacchi, R., S. Hohmann, and J. Nielsen. 2006. Yeast systems biology to unravel the network of life. *Yeast* 23:227-238.
114. Castrillo, J.I., and S.G. Oliver. 2004. Yeast as a touchstone in post-genomic research: Strategies for integrative analysis in functional genomics. *Journal of Biochemistry and Molecular Biology* 37:93-106.
115. Ideker, T., T. Galitski, and L. Hood. 2001. A NEW APPROACH TO DECODING LIFE: Systems Biology. *Annual Review of Genomics and Human Genetics* 2:343-372.
116. Armour, C.D., and P.Y. Lum. 2005. From drug to protein: Using yeast genetics for high-throughput target discovery. *Current Opinion in Chemical Biology* 9:20-24.
117. Parsons, A.B., R.L. Brost, H. Ding, Z. Li, C. Zhang, B. Sheikh, G.W. Brown, P.M. Kane, T.R. Hughes, and C. Boone. 2004. Integration of chemical-genetic and genetic interaction data links bioactive compounds to cellular target pathways. *Nature Biotechnology* 22:62-69.
118. Giaever, G., D.D. Shoemaker, T.W. Jones, H. Liang, E.A. Winzeler, A. Astromoff, and R.W. Davis. 1999. Genomic profiling of drug sensitivities via induced haploinsufficiency. *Nature Genetics* 21:278-283.
119. Giaever, G., P. Flaherty, J. Kumm, M. Proctor, C. Nislow, D.F. Jaramillo, A.M. Chu, M.I. Jordan, A.P. Arkin, and R.W. Davis. 2004. Chemogenomic profiling: Identifying the functional interactions of small molecules in yeast. *Proceedings of the National Academy of Sciences of the United States of America* 101:793-798.
120. Parsons, A.B., A. Lopez, I.E. Givoni, D.E. Williams, C.A. Gray, J. Porter, G. Chua, R. Sopko, R.L. Brost, C.H. Ho, J. Wang, T. Ketela, C. Brenner, J.A. Brill, G.E. Fernandez, T.C. Lorenz, G.S. Payne, S. Ishihara, Y. Ohya, B. Andrews, T.R. Hughes, B.J. Frey, T.R. Graham, R.J. Andersen, and C. Boone. 2006. Exploring the Mode-of-Action of Bioactive Compounds by Chemical-Genetic Profiling in Yeast. *Cell* 126:611-625.
121. Whitehead, S.N., W. Hou, M. Ethier, J.C. Smith, A. Bourgeois, R. Denis, S.A.L. Bennett, and D. Figeys. 2007. Identification and quantitation of changes in the platelet activating factor family of glycerophospholipids over the course of neuronal differentiation by high-performance liquid chromatography electrospray ionization tandem mass spectrometry. *Analytical Chemistry* 79:8539-8548.
122. Memarian, N., M. Jessulat, J. Alirezaie, N. Mir-Rashed, J. Xu, M. Zareie, M. Smith, and A. Golshani. 2007. Colony size measurement of the yeast gene deletion strains for functional genomics. *BMC Bioinformatics* 8:
123. Bonin, F., S.D. Ryan, L. Migahed, F. Mo, J. Lallier, D.J. Franks, H. Arai, and S.A.L. Bennett. 2004. Anti-apoptotic actions of the platelet-activating factor

acetylhydrolase I Î±2 catalytic subunit. *Journal of Biological Chemistry* 279:52425-52436.

124. Bligh, E.G., and W.J. Dyer. 1959. A rapid method of total lipid extraction and purification. *Can. J. Biochem. Physiol* 37:911-917.
125. Longtine, M.S., A. McKenzie Iii, D.J. Demarini, N.G. Shah, A. Wach, A. Brachat, P. Philippsen, and J.R. Pringle. 1998. Additional modules for versatile and economical PCR-based gene deletion and modification in Saccharomyces cerevisiae. *Yeast* 14:953-961.
126. Gietz, R.D., and R.H. Schiestl. 2007. High-efficiency yeast transformation using the LiAc/SS carrier DNA/PEG method. *Nature Protocols* 2:31-34.
127. Amberg, D.C. 1998. Three-dimensional imaging of the yeast actin cytoskeleton through the budding cell cycle. *Molecular Biology of the Cell* 9:3259-3262.
128. Adams, A.E.M., and J.R. Pringle. 1984. Relationship of actin and tubulin distribution to bud growth in wild-type and morphogenetic-mutant Saccharomyces cerevisiae. *Journal of Cell Biology* 98:934-945.
129. Zettel, M.F., L.R. Garza, A.M. Cass, R.A. Myhre, L.A. Haizlip, S.N. Osadebe, D.W. Sudimack, R. Pathak, T.L. Stone, and M. Polymenis. 2003. The budding index of Saccharomyces cerevisiae deletion strains identifies genes important for cell cycle progression. *FEMS Microbiology Letters* 223:253-258.
130. Lum, P.Y., C.D. Armour, S.B. Stepaniants, G. Cavet, M.K. Wolf, J.S. Butler, J.C. Hinshaw, P. Garnier, G.D. Prestwich, A. Leonardson, P. Garrett-Engele, C.M. Rush, M. Bard, G. Schimmack, J.W. Phillips, C.J. Roberts, and D.D. Shoemaker. 2004. Discovering Modes of Action for Therapeutic Compounds Using a Genome-Wide Screen of Yeast Heterozygotes. *Cell* 116:121-137.
131. Hillenmeyer, M.E., E. Fung, J. Wildenhain, S.E. Pierce, S. Hoon, W. Lee, M. Proctor, R.P. St.Onge, M. Tyers, D. Koller, R.B. Altman, R.W. Davis, C. Nislow, and G. Giaever. 2008. The chemical genomic portrait of yeast: Uncovering a phenotype for all genes. *Science* 320:362-365.
132. Botstein, D., S.A. Chervitz, and J.M. Cherry. 1997. Yeast as a model organism. *Science* 277:1259-1260.
133. Muller, E.M., N.A. Mackin, S.E. Erdman, and K.W. Cunningham. 2003. Fig1p facilitates Ca2+ influx and cell fusion during mating of Saccharomyces cerevisiae. *Journal of Biological Chemistry* 278:38461-38469.
134. Bito, H., M. Nakamura, Z. Honda, T. Izumi, T. Iwatsubo, Y. Seyama, A. Ogura, Y. Kudo, and T. Shimizu. 1992. Platelet-activating factor (PAF) receptor in rat brain: PAF mobilizes intracellular Ca2+ in hippocampal neurons. *Neuron* 9:285-294.
135. Severin, F.F., and A.A. Hyman. 2002. Pheromone induces programmed cell death in S. cerevisiae. *Current Biology* 12:R233-R235.
136. Zhang, N.N., D.D. Dudgeon, S. Paliwal, A. Levchenko, E. Grote, and K.W. Cunningham. 2006. Multiple signaling pathways regulate yeast cell death during the response to mating pheromones. *Molecular Biology of the Cell* 17:3409-3422.
137. Smotrys, J.E., M.J. Schoenfish, M.A. Stutz, and M.E. Linder. 2005. The vacuolar DHHC-CRD protein Pfa3p is a protein acyltransferase for Vac8p. *J. Cell Biol.* 170:1091-1099.

138. Bonangelino, C.J., E.M. Chavez, and J.S. Bonifacino. 2002. Genomic Screen for Vacuolar Protein Sorting Genes in Saccharomyces cerevisiae. *Mol. Biol. Cell* 13:2486-2501.
139. Huang, Y.C.T., E.S. Nozik, and C.A. Piantadosi. 1994. Superoxide dismutase potentiates platelet-activating factor-induced injury in perfused lung. *American Journal of Physiology - Lung Cellular and Molecular Physiology* 266:L246-L254.
140. Zhang, Y., Y. Gu, M.J. Lucas, and Y. Wang. 2003. Antioxidant superoxide dismutase attenuates increased endothelial permeability induced by platelet-activating factor. *Journal of the Society for Gynecologic Investigation* 10:5-10.
141. Kubes, P., M. Suzuki, and D.N. Granger. 1990. Modulation of PAF-induced leukocyte adherence and increased microvascular permeability. *American Journal of Physiology - Gastrointestinal and Liver Physiology* 259:G859-G864.
142. Schwappach, J.R., J.G. Wood, and L.Y. Cheung. 1995. Superoxide dismutase attenuates effects of platelet-activating factor on gastric microcirculation. *Journal of Surgical Research* 59:733-738.
143. Schmidt, P.J., M. Ramos-Gomez, and V.C. Culotta. 1999. A gain of superoxide dismutase (SOD) activity obtained with CCS, the copper metallochaperone for SOD1. *J Biol Chem* 274:36952-36956.
144. Akisu, M., N. Kultursay, I. Coker, and A. Huseyinov. 1998. The Effect of L-Carnitine on Platelet Activating Factor Concentration in the Immature Rat Model of Hypoxic-Ischemic Brain Injury. *Acta Medica Okayama* 52:183-187.
145. Lee, J., B. Lee, D. Shin, S.S. Kwak, J.D. Bahk, C.O. Lim, and D.J. Yun. 2002. Carnitine uptake by AGP2 in yeast Saccharomyces cerevisiae is dependent on Hog1 MAP kinase pathway. *Mol Cells* 13:407-412.
146. Nakaseko, Y., and M. Yanagida. 2001. Cell biology: Cytoskeleton in the cell cycle. *Nature* 412:291-292.
147. McLaughlin, N.J.D., A. Banerjee, M.R. Kelner, F. Gamboni-Robertson, C. Hamiel, F.R. Sheppard, E.E. Moore, and C.C. Silliman. 2006. Platelet-activating factor-induced clathrin-mediated endocytosis requires Î²-arrestin-1 recruitment and activation of the p38 MAPK signalosome at the plasma membrane for actin bundle formation. *Journal of Immunology* 176:7039-7050.
148. Newpher, T.M., R.P. Smith, V. Lemmon, and S.K. Lemmon. 2005. In vivo dynamics of clathrin and its adaptor-dependent recruitment to the actin-based endocytic machinery in yeast. *Developmental Cell* 9:87-98.
149. Lew, D.J., and D.J. Burke. 2003. The Spindle Assembly and Spindle Position Checkpoints. *Annual Review of Genetics* 37:251-282.
150. Roberts, C.J., B. Nelson, M.J. Marton, R. Stoughton, M.R. Meyer, H.A. Bennett, Y.D. He, H. Dai, W.L. Walker, T.R. Hughes, M. Tyers, C. Boone, and S.H. Friend. 2000. Signaling and circuitry of multiple MAPK pathways revealed by a matrix of global gene expression profiles. *Science* 287:873-880.
151. Tanaka, T., M. Iimori, H. Tsukatani, and A. Tokumura. 1994. Platelet-aggregating effects of platelet-activating factor-like phospholipids formed by oxidation of phosphatidylcholines containing an sn-2-polyunsaturated fatty acyl group. *Biochimica et Biophysica Acta - Lipids and Lipid Metabolism* 1210:202-208.

152. Loukin, S.H., C. Kung, and Y. Saimi. 2007. Lipid perturbations sensitize osmotic down-shock activated Ca2+ influx, a yeast "deletome" analysis. *FASEB J.* 21:1813-1820.

CONTRIBUTIONS OF COLLABORATORS

Eric Imbeault-Fréchette did the first replica of the haploid screen and I had taken his saved pictures and scored the screen my self. He also determined the concentration to use for that screen by spot assays. Dr. Shawn Whitehead performed the lipid extractions on my yeast samples and gave the extracts to Weimin (David) Hou who ran those samples on the Mass Spectrometer. David gave me the data files and I analyzed them using the Analyst software. Ying Fong helped me in the development of a computerized scoring method for the robotic screens. I supplied Dr. Jenny Brian (UBC biostatistics) with the raw data for all my automated yeast growth curves and she used the R programming language to normalize, curve fit, and assess statistical significance of the curves. The results of her work are not presented here.

CV

Education

- ***Masters in Biochemistry – training in Systems Biology*** **2006 - 2008**
  University of Ottawa, Ottawa
  - Thesis *topic*: "Chemo-genomic profiling of Platelet-Activating Factor in Yeast." – studying neurodegeneration via model organisms!

- ***B.Sc. Honours in Biochemistry and Biotechnology*** **2002 - 2006**
  Carleton University, Ottawa
  - Honours Thesis *topic*: "Assessment of a modified Diatomaceous Earth's binding to and filtration of microbes and bacteriophage."

Work Experience

- **Summer Student** ***Summer of 2005***
  Dr. Myron Smith's Lab, Carleton University
  - Full-time R&D on the Celite® material in collaboration with EcoVuAnalytics™.
  - Assessed Celite's ability to adsorb bioluminescent bacteria and Lambda phage for the purpose of developing a drinking-water *filter* and analysis tool.
  - Presented updates to lab members, Dr. Myron, and EcoVuAnalytics™.

- **Intern** ***Summer of 2004***
  Kemiatech™
  - Part-time R&D in the production, assessment, and quality testing of shampoo pearlizer and soaps.
  - Helped in product development and formulae testing.

Skills

Practical Laboratory Expertise

Cell Biology:
- Immunofluorescence
- Mammalian Cell Culture
- Cell Viability
- Flow cytometry

Molecular Biology:
- Real-time PCR

Biochemistry:
- SDS-PAGE and immunoblot analyses
- Quantitation of proteins
- Enzyme kinetics
- Gradient centrifugation
- Tube dialysis and lyophilization
- Isoelectric focusing

- DNA extraction
- Plasmid DNA prep
- Yeast Genomics and Y2H

Analytical Chemistry:

- GC and HPLC
- FT-IR
- Other chromatography methods

Inventiveness and taking Initiative

- Develop methods that speed up data analysis.
- Helped develop a computerized way to analyze chemo-genomic screens.
- Setup a plasmid database and trained lab members to use it.
- Developed growth methods for yeast and optimized them for flow cytometry and other applications.

Computer Proficiency

- Word, Excel, Outlook, Photoshop, Osprey/cytoscape, Blast, Cluster Treeview, VNTI, Chromas, SPDBV, Populus, Analyst 1.4.1, ClustalW, and Volocity.
- Visual Basic and C++.
- Applied PHP programming for Bioinformatics at CarletonU.
- Wrote MS Excel *macros* to facilitate *data analysis* during M.Sc.

Other Training

- Leica fluorescence microscope.
- Fire Safety, Lab Safety, and Biosafety.
- WHMIS, Autoclave, and Centrifuge Training.
- Singer RoTor HDA robot training.
- Beckman Coulter FC500 Flow Cytometer
- Thermo 96-well plate-reader.

Awards

- The Graham Walker Summer Student Research Award (April 2005)
- Dean's List in 2003 and Presidents Entrance Scholarship in 2002 and 2003
- Awarded *Youth Leadership Award* by US Congressional Leadership Council.

Affiliations

- Member of Canadian Society for Systems Biology (CSSB)